Charles University
Faculty of Mathematics and Physics
Department of Chemical Physics and Optics

HABILITATION THESIS

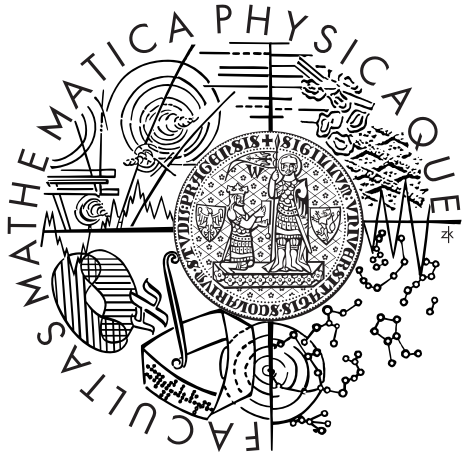

LUCIE D. AUGUSTOVIČOVÁ

QUANTUM DYNAMICS OF SMALL MOLECULAR SYSTEMS FROM DIATOMICS TO POLYATOMICS

Prague 2020

ACKNOWLEDGMENTS

At the first place, I address my deepest thanks to my husband, and my whole family for their understanding and endless love, their support and patience during my years of research.

I am also grateful to all my colleagues and students I worked with at Charles University in Prague, at Czech Academy of Sciences, at Max-Planck-Institute of Astrophysics MPG in Garching, Germany, at JILA, National Institute of Standards and Technology and at University of Colorado in the USA.

I thank my colleague and former advisor Pavel Soldán for bringing me to the vast and interesting field of atomic and molecular physics in which I met wonderful collaborators and friends, especially Vladimír Špirko, Wolfgang P. Kraemer, people from group of Juraj Glosík and foremost John L. Bohn with whom I could spend two splendid years in Boulder and whom I am still regularly visiting as well as my beloved adoptive family.

My work was financially supported by the Grant Agency of the Czech Republic, the Grant Agency of the Charles University, the US National Science Foundation, the US Army Research Office, and by the JILA NSF Physics Frontier Center as acknowledged in the published papers.

LIST OF PUBLICATIONS

PUBLICATIONS IN SCIENTIFIC JOURNALS WITH IF

Augustovičová, L. D. and J. L. Bohn (2017). "No evaporative cooling of nitric oxide in its ground state." In: *Physical Review A* 96, p. 042712.
DOI: 10.1103/PhysRevA.96.042712.

Augustovičová, L. D. and J. L. Bohn (2018a). "Manifestation of quantum chaos in Fano-Feshbach resonances." In: *Physical Review A* 98, p. 023419.
DOI: 10.1103/PhysRevA.98.023419.

Augustovičová, L. D. and J. L. Bohn (2018b). "NO evaporative cooling in the $^2\Pi_{3/2}$ state." In: *Physical Review A* 97, p. 062703.
DOI: 10.1103/PhysRevA.97.062703.

Augustovičová, L. D. and J. L. Bohn (2019). "Ultracold collisions of polyatomic molecules: CaOH." In: *New Journal of Physics* 21.10, p. 103022.
DOI: 10.1088/1367-2630/ab4720.

Augustovičová, L. D. and J. L. Bohn (2020). "Ultracold collisions of the lithium monoxide radical." In: submitted.

Augustovičová, L., W. P. Kraemer, and P. Soldán (2014a). "Depopulation of metastable helium by radiative association with hydrogen and lithium ions." In: *The Astrophysical Journal* 782, 46.
DOI: 10.1088/0004-637X/782/1/46.

Augustovičová, L., W. P. Kraemer, and P. Soldán (2014b). "Depopulation of metastable helium He(2^1S) by radiative association with hydrogen and lithium cations." In: *Journal of Quantitative Spectroscopy and Radiative Transfer,* 148, pp. 27–37.
DOI: 10.1016/j.jqsrt.2014.06.012.

Augustovičová, L., W. P. Kraemer, V. Špirko, and P. Soldán (2015a). "The role of molecular quadrupole transitions in the depopulation of metastable helium." In: *Monthly Notices of the Royal Astronomical Society* 446, pp. 2738–2743.
DOI: 10.1093/mnras/stu2317.

Augustovičová, L. and P. Soldán (2012). "Ab initio properties of MgAlk (Alk = Li, Na, K, Rb, Cs)." In: *Journal of Chemical Physics* 136, 084311.
DOI: 10.1063/1.3690459.

Augustovičová, L., P. Soldán, W. P. Kraemer, and V. Špirko (2014c). "Potential microwave probes of the proton-to-electron mass ratio

at very high redshifts." In: *Monthly Notices of the Royal Astronomical Society* 439, pp. 1136–1139.
DOI: 10.1093/mnras/stu060.

Augustovičová, L., P. Soldán, W. P. Kraemer, and V. Špirko (2014d). "Potential microwave probes of the proton-to-electron mass ratio at very high redshifts (supplementary material)." In: *Monthly Notices of the Royal Astronomical Society*, pp. 1–8.
DOI: 10.1093/mnras/stu060.

Augustovičová, L., P. Soldán, and V. Špirko (2016). "Effective hyperfine structure functions of ammonia." In: *The Astrophysical Journal* 824, p. 147.
DOI: 10.3847/0004-637x/824/2/147.

Augustovičová, L., V. Špirko, W. P. Kraemer, and P. Soldán (2012a). "Radiative association of $LiHe^+$." In: *Chemical Physics Letters* 531, pp. 59–63.
DOI: 10.1016/j.cplett.2012.02.038.

Augustovičová, L., V. Špirko, W. P. Kraemer, and P. Soldán (2013a). "Radiative association of He_2^+ revisited." In: *Astronomy & Astrophysics* 553, A42.
DOI: 10.1088/0004-637X/749/1/22.

Augustovičová, L., V. Špirko, W. P. Kraemer, and P. Soldán (2013b). "Radiative association of He_2^+: the role of quartet states." In: *Monthly Notices of the Royal Astronomical Society* 435, pp. 1541–1546.
DOI: 10.1093/mnras/stt1395.

Augustovičová, L. D. and V. Špirko (2020a). "Morphing radial molecular property functions of hydroxyl." In: submitted.

Augustovičová, L. D. and V. Špirko (2020b). "Zeeman molecular probe for tests of fundamental physical constants." In: *Monthly Notices of the Royal Astronomical Society* 494.2, pp. 1675–1680.
DOI: 10.1093/mnras/staa792.

Augustovičová, L., M. Zámečníková, W. P. Kraemer, and P. Soldán (2015b). "Radiative association of $He(2^3P)$ with lithium cations." In: *Chemical Physics* 462. Inelastic Processes in Atomic, Molecular and Chemical Physics, pp. 65–70.
DOI: 10.1016/j.chemphys.2015.07.003.

Belyaev, A. K., L. Augustovičová, P. Soldán, and W. P. Kraemer (2014). "Non-radiative inelastic processes in lithium-helium ion-atom collisions." In: *Astronomy & Astrophysics* 565, A106.
DOI: 10.1051/0004-6361/201423578.

Belyaev, A. K., D. S. Rodionov, L. Augustovičová, P. Soldán, and W. P. Kraemer (2015). "Full quantum study of non-radiative inelastic processes in lithium-helium ion-atom collisions." In: *Monthly Notices of the Royal Astronomical Society* 449, pp. 3323–3332.
DOI: 10.1093/mnras/stv391.

Glosík, J., P. Dohnal, Á. Kálosi, L. D. Augustovičová, D. Shapko, Š. Roučka, and R. Plašil (2017). "Electron-ion recombination in low temperature hydrogen/deuterium plasma." In: *The European Physical Journal Applied Physics* 80, p. 30801.
DOI: 10.1051/epjap/2017170228.

Kálosi, Á., P. Dohnal, L. Augustovičová, Š. Roučka, R. Plašil, and J. Glosík (2016). "Monitoring the removal of excited particles in He/Ar/H2 low temperature afterglow plasma at 80-300 K." In: *The European Physical Journal Applied Physics* 75, p. 24707.
DOI: 10.1051/epjap/2016150587.

Shapko, D., P. Dohnal, M. Kassayová, Á. Kálosi, S. Rednyk, Š. Roučka, R. Plašil, L. D. Augustovičová, et al. (2020). "Dissociative recombination of N2H+ ions with electrons in the temperature range of 80–350 K." In: *The Journal of Chemical Physics* 152.2, p. 024301.
DOI: 10.1063/1.5128330.

OTHER PEER-REVIEW PUBLICATIONS (REGISTERED IN THE WOS/ISI DATABASE)

Zámečníková, M., L. Augustovičová, W. P. Kraemer, and P. Soldán (2015). "Formation of molecular ion $LiHe^+$ by radiative association of metastable helium $He(2^3P)$ with lithium ions." In: *Journal of Physics: Conference Series* 635, p. 022038.
DOI: 10.1088/1742-6596/635/2/022038.

CONTENTS

SUMMARY OF NOTATION

Scalar quantities and variables, and symbols for constants are written in upright glyphs (Latin or Greek), as a, b, c, π. Vector quantities are printed in boldface as $\mathbf{L}, \mathbf{S}, \mathbf{J}$ and their quantum numbers are denoted by the same letters in upright glyphs: L, S, J. The meanings of some common symbols used throughout the text are listed below. More specific quantities are explained directly in the text. Prime or double prime is used to distinguish the upper ($'$) and lower ($''$) levels in a transition. They occur as superscripts on the quantum numbers. The subscripts g or u indicate the molecular states associated with the gerade (even) or ungerade (odd) symmetry, respectively.

v	vibrational quantum number
E	energy
$\mathbf{L}$	orbital angular momentum
$\mathbf{S}$	electron spin angular momentum
$\mathbf{J}$	total angular momentum excluding nuclear spin
$\mathbf{N}$	total angular momentum excluding electron and nuclear spin, in the case where electron spin is present
$\mathbf{I}$	nuclear spin angular momentum
$\mathbf{F}$	total angular momentum including electron and nuclear spin
Λ	projection of $\mathbf{L}$ along internuclear axis (body-fixed projection)
Σ	projection of $\mathbf{S}$ along internuclear axis (body-fixed projection)
$\Omega = \Lambda + \Sigma$	projection of total electronic angular momentum along internuclear axis
M	projection of $\mathbf{J}$ on the space-fixed quantization axis
k	projection of $\mathbf{J}$ along the intermolecular z-axis
K	unsigned projection quantum number $K = \lvert k \rvert$
Σ, Π, Δ	electronic state designation for which $\lvert\Lambda\rvert = 0, 1, 2$, respectively
(ϕ, θ, γ)	Euler angles
k_B	Boltzmann constant
R	internuclear distance
R_e	equilibrium internuclear distance
$U(R)$	potential energy curve

ϵ_0	permittivity of vacuum
μ_0	permeability of vacuum
c	speed of light in vacuum
T	temperature
μ	reduced mass

The formulas presented in this thesis are reported in SI units unless explicitly noted otherwise; the exceptions to this rule are spectroscopic properties and characteristics (such as distances, e.g.), which are normally reported in atomic units (a.u.). Energies are here most frequently reported in K, cm^{-1} or in eV. In the atomic units system, four frequently used quantities (Planck's constant h divided by 2π [$\hbar$], elementary charge [e], electron mass [m_e], and inverse Coulomb's constant [$4\pi\epsilon_0$]) are all unity by definition, making formulas more simple to read. The atomic unit of length is the *bohr*

$$a_0 = \frac{4\pi\epsilon_0\hbar^2}{m_e e^2},$$

where $a_0 \approx 0.529\,177\,210\,92(17) \times 10^{-10}$m.
The atomic unit of energy is the *hartree*

$$E_h = \frac{e^2}{4\pi\epsilon_0 a_0},$$

and it has the value $E_h \approx 4.359\,744\,722\,2071(85) \times 10^{-18}$ J , or $E_h/(hc) \approx 2.194\,746\,313\,6320(43) \times 10^5\,cm^{-1}$. Units for other quantities can be readily worked out from these basic few.

PREFACE

The main scientific results of the research that I carried out in the years 2014–2020 are written up in this habilitation thesis. This is mirrored in the selected publications that can be found in the attachment to this thesis. The covered topics encompass broad field of molecular physics of small systems, ranging from radiative and non-radiative processes in early Universe, stellar environments and interstellar medium, through quantum studies on possible cosmological variation of fundamental constants to physics of ultracold molecules and quantum chaos. Therefore, the main part of this thesis is divided into four fundamental chapters according to their focus. The purpose of this work is to briefly describe the current state and summarize the author's contributions to these issues.

This thesis is organized as follows: it consists of two parts, the topical overview of my research followed by the attached scientific papers, available only in the printed version.

Chapter 1 gives an introduction to radiative processes and discusses its importance for astrochemistry together with a review of relevant literature. This is followed by a theoretical description of the transition processes forming molecular ions or deexcitation of collisional partners, and a summary of main results and findings.

In Chapter 2 the critical exploration of the possibility that the fundamental constants of nature may depend on time and space in the evolving Universe is considered. The possibility of using spectra of light homonuclear molecular ions, ammonia isotopomers or diatomic hydride radicals as potential probes of the variations of the proton-to-electron mass ratio is investigated.

Chapter 3 focuses on the possibility of cooling polar molecules to nanoKelvin temperature range. The ultracold collisions of several molecular systems are investigated with emphasis on the influence of external electric or magnetic field on elastic or inelastic collisional rates.

Chapter 4 summarizes the results on the emergence of quantum chaos in collisions of ultracold magnetic lanthanide atoms. In this systems quantum chaos is manifested in Fano-Feshbach resonances due to dense distribution of levels near the dissociation threshold of the formed dimer.

A summary of the main results and findings of this thesis as well as conclusion and outlook can be found in Chapter 5.

All relevant papers, published in peer-reviewed international scientific journals with impact factor, of which I am the main author or a coauthor are attached in the appendices.

OVERVIEW OF SELECTED TOPICS IN MY RESEARCH

Proti trampotám života dal Bůh člověku tři věci - naději, spánek a smích.

— Immanuel Kant

1

RADIATIVE PROCESSES IN ASTROCHEMISTRY

The first chapter is dedicated to the study of quantum dynamics of radiative processes in molecules and molecular ions with astrophysical importance. Such processes include spontaneous emission, emission and absorption stimulated by black-body radiation, and radiative association. All these processes have to be taken into account when studying wide range of phenomena from the past and present, e.g. the physical and chemical processes involved in the formation and evolution of interstellar molecules (Tielens, 2013). Of particular importance is the formation of the first molecules in the Universe (Lepp et al., 2002). The computational approach developed for calculation of radiative processes in molecules is useful even for the search for the possible space-time variations of fundamental constants (Augustovičová et al., 2014c) as will be demonstrated in Chapter 2.

One important avenue of research is focused on the growth of molecular complexity in the early Universe, when after the period of fast initial expansion a decrease in number densities and temperature occurred, ending nucleosynthesis. During the recombination epoch, the neutral atoms He, H and D and singly charged ions He^+ and Li^+ were produced in collisions of H^+, D^+, He^{2+} and Li^{3+} with electrons. With the formation of the very first neutral atom – helium – the creation of the first molecular ions (HeH^+ and then H_2^+ (Lepp et al., 2002)) could proceed via spontaneous radiative association process (and at the same time be enhanced due to a stimulating background radiation field). It is interesting to note that, although HeH^+ was a cornerstone of early Universe chemistry, it was detected only recently (Güsten et al., 2019) in planetary nebula NGC 7027. The subsequent formation of the neutral H_2 molecule (via charge transfer reaction of H_2^+ with H (Lepp et al., 2002) and at later times through associative detachment reaction of H^- with H (Kreckel et al., 2010; Gerlich et al., 2012)) led to cooling of primordial clouds allowing them to collapse. Thus the radiative association stands at the beginning of the chain of processes leading to the formation of the first structures in the early Universe. Hydrogen and helium containing diatomic ions H_2^+, HeH^+ and He_2^+ are assumed to be present in significant abundances in the atmospheres of white dwarf stars, either in the helium-rich ones or in the more numerous hydrogen-dominated DA-type stars, respectively (Koester and Chanmugam, 1990).

In addition to cooling, radiation due to spontaneous depopulation has important astrophysical implications, as metastable atomic states are considered to provide most of the light emitted from planetary nebulae. The measured intensities of the relevant radiation lines can yield information on temperatures, densities and chemical compositions in these environments.

Helium is an important atomic species for primordial chemistry with cosmic abundance second only to hydrogen. Its metastable triplet state He 2^3S with electronic configuration 1s2s (19.75 eV above the helium ground state) has an extremely long lifetime - about two hours (Drake, 1971; Hodgman et al., 2009) because the direct radiative transition to the ground state is doubly forbidden by quantum mechanical selection rules. The relatively large amount of helium in interstellar space, led the author and her co-workers to study the depopulation of the metastable levels (both singlet and triplet) of He by radiative collisions with hydrogen, helium and lithium ions - i.e. species present in abundance in early Universe. These collisions result in the formation of molecular cations, either in high-spin or low-spin electronic state through the process of radiative association.

Radiative association reaction proceeds through collision of two smaller species that can remain close together for a considerable time and form an unstable collisional complex even on the excited state potentials. The barrier that holds the two species (either ion-atom pairs or reactive neutrals) together is most commonly caused by centrifugal potential, but there are many adiabatic potential curves which exhibit barriers even for zero angular momentum. Stabilization of the complex against redissociation is finally ensured by radiative transition to bound levels of the ground or other lower-lying electronic state.

Studies of collisional complexes on different excitation levels can provide reaction rates crucial for the primordial and interstellar chemistry, especially when the efficiencies of radiative processes at different temperatures are compared. Due to the difficulty of corresponding laboratory experiments (Gerlich and Horning, 1992), most of the cross sections and rate coefficients for radiative association processes must be obtained by theoretical methods, although in recent years there was a promising development in experimental techniques for radiative association rate coefficient determination (Beyer and Merkt, 2018).

Radiative association was proposed as an effective formation mechanism in the interstellar medium already in the early forties (Swings, 1942). Bates (Bates and Spitzer, 1951; Bates, 1951) derived a semiclassical formula for the cross sections based on the unrestricted transition rate and calculated the rate coefficients for radiative association of CH, CH^+, N_2^+ and H_2^+.

Building on the results of these pioneering studies were groups of Dalgarno (e. g. Stancil et al., 1993; Babb and Dalgarno, 1995; Dalgarno

et al., 1996; Zygelman et al., 1998), Dickinson (e. g. Bennett et al., 2003; Dickinson, 2005), Gianturco (e. g. Gianturco and Giorgi, 1996; Gianturco and Giorgi, 1997; Bovino et al., 2011), Talbi (e. g. Bacchus-Montabonel and Talbi, 1999; Talbi and Bacchus-Montabonel, 2007), Kraemer and Špirko (e. g. Juřek et al., 1995; Mrugała et al., 2003; Mrugała and Kraemer, 2005) and others who performed thorough investigations on radiative association of various species.

My theoretical work focused on simple interacting systems such as He + H^+, He + He^+, Li^+ + He, Li + He^+, and similar. The choice of considered systems was governed mainly by the importance of the corresponding reactions for astrophysics and chemistry of the early Universe.

I and my collaborators have published a number of detailed studies of spontaneous and stimulated radiative association of molecular ions HeH^+, $LiHe^+$, and He_2^+ (Augustovičová et al., 2012; Augustovičová et al., 2013a; Augustovičová et al., 2013b; Augustovičová et al., 2014a; Augustovičová et al., 2014b; Augustovičová et al., 2015a; Augustovičová et al., 2015b; Zámečníková et al., 2015). The theoretical framework will be introduced further followed by a section giving a description and discussion of selected results.

1.1 METHODOLOGY

Disclaimer: This section may contain similarities with my dissertation thesis (Augustovičová, 2014). Text coincidence in definitions, formulas, *termini technici*, methods, or references to earlier works in this field is hard to avoid.

Continuous-bound transitions

The reactive processes occurring in ion-atom collisions include two possibilities: Either a (positive) charge is transferred from an ion to an atom (or molecule), the respective reaction is referred to as a charge transfer reaction, or the reaction results in molecule/molecular ion formation in the radiative association process. The energy conservation is maintained by a transition accompanied by the emission of a photon of energy.

In quantum mechanics, the total cross sections $\sigma(E; T_b)$ for radiative association of a diatomic bound species in the field of blackbody radiation (characterized by temperature T_b) can be expressed as a sum of the partial cross sections over allowed transitions between a continuum state with a positive energy E and orbital angular momentum J' to bound ro-vibrational states (labeled by vibrational quantum number v'' and orbital angular momentum J'') (Zygelman and Dalgarno, 1990). Each of such contributions corresponds to a

radiative-association cross section from the channel E, J' towards the level v'', J'' being expressed as (Stancil and Dalgarno, 1997)

$$\sigma^{\text{dip.}}_{J';v'',J''}(E;T_b) = \frac{1}{4\pi\epsilon_0}\frac{64}{3}\frac{\pi^5}{c^3\,k^2}\,p\,\nu^3_{E;v'',J''}\,\mathcal{S}^{\text{dip.}}_{J',J''}\,M^2_{E,J';v'',J''} \quad \times \\ \times\left[\frac{1}{1-\exp\left[-h\nu_{E;v'',J''}/(k_B T_b)\right]}\right] \tag{1}$$

for transitions driven by dipole moment and

$$\sigma^{\text{quad.}}_{J';v'',J''}(E;T_b) = \frac{1}{4\pi\epsilon_0}\frac{32}{5}\frac{\pi^7}{c^5\,k^2}\,p\,\nu^5_{E;v'',J''}\,\mathcal{S}^{\text{quad.}}_{J',J''}\,M^2_{E,J';v'',J''} \quad \times \\ \times\left[\frac{1}{1-\exp\left[-h\nu_{E;v'',J''}/(k_B T_b)\right]}\right] \tag{2}$$

for transitions driven by quadrupole moment.

The variables in this formula represent: c the speed of light in vacuum, the wave number k of the scattered particle is related to the relative energy E by $k^2 = 2\mu E/\hbar^2$, μ is the reduced mass of the molecular species, p is the probability in the input channel, $\nu_{E;v'',J''}$ the emitted photon frequency, $h\nu_{E;v'',J''} = E + \triangle E - E_{v'',J''}$, where $\triangle E$ is the difference in energies of the initial collision partners in an infinity distance and of the dissociation products of the final electronic states, and

$$M_{E,J';v'',J''} = \int_0^\infty \chi_{J'}(E,R)\,T^\kappa_{|\sigma|}(R)\,\psi_{v'',J''}(R)\,dR \tag{3}$$

is the transition matrix element of the irreducible spherical tensor operator $T^\kappa_{|\sigma|}$ of rank κ, $\sigma = -\kappa,\ldots,\kappa$, (the dipole moment operator μ_m has rank 1; $\sigma = 0$ for the $\Sigma-\Sigma$ transitions and $\sigma = \pm 1$ for the $\Pi-\Sigma$ transitions, the quadrupole moment Q_m has rank 2; $\sigma = 0$ for the $\Sigma-\Sigma$ transitions considered here) between the initial continuum energy-normalized radial wave function $\chi_{J'}(E,R)$ for the partial wave J' and the final $\mathcal{L}^2$-normalized bound-state radial wave function $\psi_{v'',J''}(R)$. The wave functions $\chi_{J'}(E,R)$ and $\psi_{v'',J''}(R)$ were calculated by numerical integration of the corresponding radial Schrödinger equations using the Numerov-Cooley method (Numerov, 1923; Cooley, 1961).

Finally, $\mathcal{S}_{J',J''}$ are the rotational line strength factors (so-called Hönl-London coefficient) for a dipole/quadrupole transition governed by the rotational selection rules for $\triangle J = J' - J''$. They were derived and reported in Augustovičová, 2011 for the nine and fifteen possible types of linear Hund's case (a) molecules transitions. In particular, for $\Sigma^\pm - \Sigma^\pm$

$$\mathcal{S}^{\text{dip.}}_{J',J'+1} = J' + 1,\ \mathcal{S}^{\text{dip.}}_{J',J'-1} = J', \tag{4}$$

and

$$\mathscr{S}^{\text{quad.}}_{J',J'} = \frac{(2J'+1)J'(J'+1)}{(2J'-1)(2J'+3)},\ \mathscr{S}^{\text{quad.}}_{J',J'+2} = \frac{3}{2}\frac{(J'+1)(J'+2)}{2J'+3},$$

$$\mathscr{S}^{\text{quad.}}_{J',J'-2} = \frac{3}{2}\frac{J'(J'-1)}{2J'-1}, \tag{5}$$

where the superscript denotes dipole/quadrupole transition, respectively. Note that a set of Hönl-London factors for an allowed ${}^{2S'+1}\Lambda' - {}^{2S''+1}\Lambda''$ transition connected to a given J' (or J'') obey a standard sum rule

$$\sum \mathscr{S}_{J',J''} = (2-\delta_{0\Lambda'}\delta_{0\Lambda''})(2S+1)(2J+1)\,, \tag{6}$$

with the sum over all $\triangle J$ and any Λ-doublets (Bernath, 2005).

The rate constants for formation of a molecule by (spontaneous $T_b = 0$ and stimulated) radiative association at temperature T are then derived from the total cross sections $\sigma(E;T_b) = \sum \sigma_{J';v'',J''}(E;T_b)$ by averaging over a Maxwellian velocity distribution of the collisional continuum

$$\alpha(T;T_b) = \left(\frac{8}{\mu\pi}\right)^{1/2}\left(\frac{1}{k_B T}\right)^{3/2}\int_0^\infty E\,\sigma(E;T_b)\,e^{-E/k_B T}dE, \tag{7}$$

assuming that the system is found in thermodynamic equilibrium.

We improved the theoretical approach of Dalgarno and coworkers (Zygelman and Dalgarno, 1990; Stancil and Dalgarno, 1997) by taking into account the numbers of shape resonances, which are not negligible in some studied processes, in order to evaluate this integral as accurately as possible. In the actual calculation the total reaction rates can be obtained by summing over all resonant and non-resonant contributions. The inclusion of these resonances in the computation can increase the RA rate coefficients by up to 15 % (Augustovičová et al., 2012). The resonance partial-wave J'_r contribution is counted in the rate coefficient calculation according to the numerical value of the ratio $\Gamma^t_{E_r,J'_r}/E_r$, where $\Gamma^t_{E_r,J'_r}$ is the resonance tunneling width and E_r is its energy position. Resonances satisfying the criterion $\Gamma^t_{E_r,J'_r} \ll E_r$ are assumed to be "narrow" and vice versa. So we follow the approach of (Augustovičová et al., 2012), where contributions from wide and narrow resonances are treated separately from the background contribution. I hope the readers will forgive me that I will not depict details about calculation of adiabatic Born-Oppenheimer molecular state potentials, dipole and quadrupole moment functions of specific electronic states of studied molecular species, bound-state, orbiting resonance and continuum wave functions as well as interpolation and extrapolation of potential curves and their molecular characteristics and refer readers to the attached publications and other Refs. (Soldán and Kraemer, 2012; Augustovičová et al., 2012; Augustovičová et al.,

2013a; Augustovičová et al., 2013b; Augustovičová et al., 2014a; Augustovičová et al., 2014b; Belyaev et al., 2015; Augustovičová et al., 2015b)

Bound-bound transitions

For ability of molecular species to electronic transitions and chemical elementary processes the knowledge of radiative lifetimes of molecular species is of key importance. While transition probabilities can be obtained indirectly by measurements of radiative lifetimes, experimental measurements of emission spectral line intensities are difficult to obtain for many high temperature molecular species. Calculated line intensities then provide an alternative to measurements burdened by systematic errors and means for calibration in experiments.

Depopulation of a given level J' with energy E' and number density $\mathcal{N}'$ (in molecules/m^3) is given in the absence of an external radiation field by the rate equation

$$\frac{d\mathcal{N}'}{dt} = -A_{f\leftarrow i}\mathcal{N}', \tag{8}$$

where the constant of proportionality $A_{f\leftarrow i}$ is the Einstein coefficient for emission. It implies that an excited-level population decays exponentially with time at rate $A_{f\leftarrow i}$. This decay rate determines the radiative lifefime of level E' as

$$(\tau_{i=E'})^{-1} = \sum_{f=E''} A_{f\leftarrow i}\,. \tag{9}$$

The Einstein A-coefficient can be approximated by the leading term in the multipole moment expansion, which can be written for electric-dipole allowed transitions as

$$A_{f\leftarrow i} = \frac{64\pi^4\nu_{if}^3}{(4\pi\varepsilon_0)3hc^3}\frac{1}{g_i}S^{dip.}_{f\leftarrow i}, \tag{10}$$

where $S^{dip.}_{f\leftarrow i}$ is the line strength of an electric dipole transition between all substates of the initial upper and final lower levels. The degeneracy factor (statistical weight) g_i of the initial state takes into account electronic, vibration, rotation, nuclear etc. statistics.

Line intensity for electric dipole transition arising between upper state with energy E' and lower state with energy E'' is given by (Bernath, 2005)

$$I_{f\leftarrow i} = \frac{8\pi^3\,\tilde{\nu}_{if}}{(4\pi\varepsilon_0)\,3hc\,Q(T)}\left[e^{-E''/k_BT} - e^{-E'/k_BT}\right]S^{dip.}_{f\leftarrow i}, \tag{11}$$

where $\tilde{\nu}_{if} = (E' - E'')/hc$ is the wavenumber of the transition (in cm^{-1}) and $Q(T)$ is the total internal partition function, which has

been scaled such that the minimum possible rotational-vibrational level has zero energy. The intensity is related to a single molecule event. Note that there are many other definitions and notations of the line intensity as numerous choices for quantities ν or $\mathcal{N}_{tot}$ (molecular number density) are possible, which causes confusion concerning units. $I_{f\leftarrow i}$ has the dimension of $cm^{-1}/(molecule\times cm^{-2})$, commonly referred to as HITRAN unit defined as wavenumber per column density (Rothman et al., 1998). This quantity is often called the integrated absorption coefficient.

Combination of Equations (11) and (10) yields a relation between the line intensity and the Einstein A-coefficient corresponding to the transition $f \leftarrow i$

$$I_{f\leftarrow i} = \frac{g_i}{Q(T)} \frac{A_{f\leftarrow i}}{8\pi c \tilde{\nu}_{if}^2} \left[e^{-E''/k_B T} - e^{-E'/k_B T} \right].$$

1.2 SUMMARY OF RESULTS IN THE ATTACHED PAPERS

The research presented in this section is based on papers that are included in the full printed version. Therefore, this section provides merely an abstract and accents high points of the obtained results. For full details I refer the reader to the appended part of this thesis that contains the corresponding papers.

In the attached papers (Augustovičová et al., 2014a; Augustovičová et al., 2014b; Augustovičová et al., 2015a; Augustovičová et al., 2015b) we investigated thoroughly the two-body association process

$$A + B \rightarrow AB^* \rightarrow AB + h\nu\,,$$

in which the collision complex AB^* is stabilized against dissociation by spontaneous emission of a photon with frequency ν. Apart from spontaneous emission, processes stimulated by the cosmic background radiation were also considered. The cosmic background radiation can enhance molecule formation by stimulated radiative association

$$A + B + h\nu_b \rightarrow AB + h\nu + h\nu_b\,,$$

where ν_b is the frequency of the background radiation field with effective temperature T_b. In this context, detailed studies of spontaneous and stimulated radiative association resulting in the formation of the HeH^+ (HeD^+), He_2^+, and $LiHe^+$ molecular ions have been performed.

These calculations were performed employing the Born-Oppenheimer approximation, and the processes studied were characterized by means of energy-dependent cross sections and temperature-dependent rate coefficients. Contrary to previous works, highly excited electronic states were also included in these studies.

Due to the eminence of considered molecules and their formation processes for astrochemistry the emphasis is on the calculation of the rate coefficients of the corresponding reactions.

Among the main outcomes of these studies were realizations that the metastable helium atoms in planetary nebulae are significantly depopulated due to spontaneous radiative association process, and that the black-body background radiation enhances radiative association rates predominantly at low collision temperatures and only for those processes with small energy of emitted photons, e.g. for inelastic processes within one electronic state (see Fig. 1). The absence of this phenomenon in the majority of two-state processes, where emitted photon frequencies are very large, is caused by the factor $[1-\exp(-h\nu_{E;v'',J''}/k_B T_b)]^{-1}$ in Eqs. (1) and (2) being almost 1. For reaction temperatures below a few thousand K the increase of rate coefficients due to black-body background radiation can be by an order of magnitude or more, for larger temperatures stimulation appears to be ineffective.

The cross sections for spontaneous ($T_b = 0$ K) and stimulated radiative association were calculated as functions of the relative collision energy of the reactants in the range of 10^{-6} and 10 eV. Typical quantum-mechanical cross sections obtained in our studies (see e.g. Fig. 2) are generally decreasing with increasing collision energy and have a rapid drop-off in the energy range between 0.1 and 10 eV. This is a typical behavior for radiative collision processes including radiative charge transfer (cf. e.g. Zygelman et al., 1989; Belyaev et al., 2014).

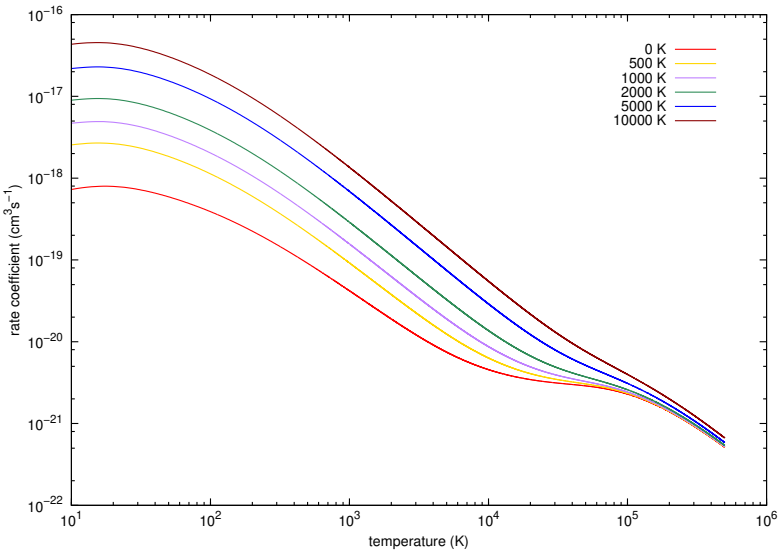

Figure 1: Adapted from Ref. Augustovičová et al. (2014b): Rate coefficients for the stimulated and spontaneous radiative association of H^+ and He(2^1S) (continuum-bound $B(^1\Sigma^+) \rightarrow B(^1\Sigma^+)$ process) at different background temperatures.

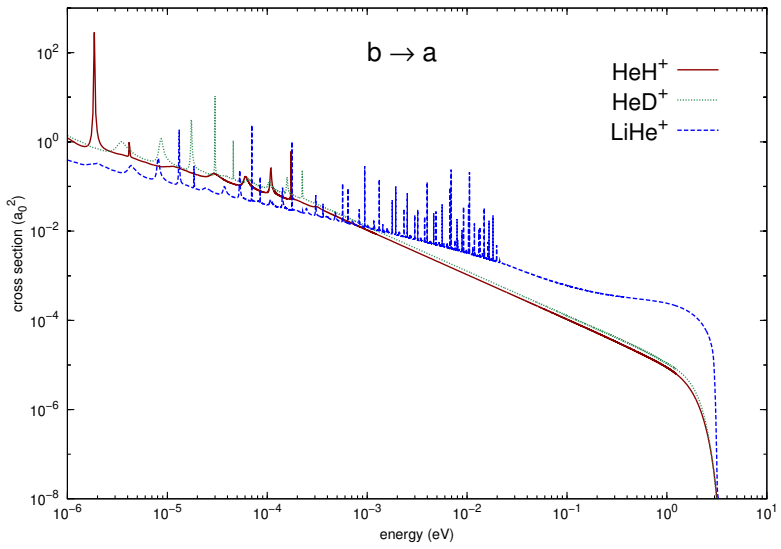

Figure 2: Adapted from Ref. Augustovičová et al. (2014a): Cross sections versus energy for spontaneous ($T_b = 0$ K) radiative association process $b(^3\Sigma^+) \rightarrow a(^3\Sigma^+)$ of formation three different molecular ions. Displayed are only the contributions of resonances with widths wider than 0.01 cm^{-1}.

The downhill background profile is usually complemented by a complex resonance structure while some of the resonance widths can be vanishingly small. Such features exceedingly complicate the numerical evaluation of the integral in Eq. (7). We bypassed this issue by treatment of wide and narrow resonance contributions to the radiative-association rate coefficients in a separate calculation following the procedure outlined in Section 1.1. For further details interested readers are referred to the Ref. (Augustovičová et al., 2012).

The low-energy resonance structure arises from the existence of quasi-bound states trapped behind centrifugal barriers in the reactant channel and is mostly determined by the depth and anharmonicity of the target potential. Provided one-state process the resonance structure is most pronounced, but for the two-state processes it is practically missing unless the final potential supports a large number of bound-state partners.

Different sizes of spontaneous cross sections, and hence rate coefficients, varying even by orders of magnitude can be attributed to the very large difference in ionization potentials of respective atomic species This can be seen e.g. in Fig. 3 in which three target molecular potentials of $LiHe^+$ are involved, or in Fig. 4 showing formation of He_2^+ via various processes. Apart from the fact that the third power of the emitted photon frequency overwhelmingly dominates the total cross section, the number of terms in the sum of partial cross sections that is determined by the number of target rovibra-

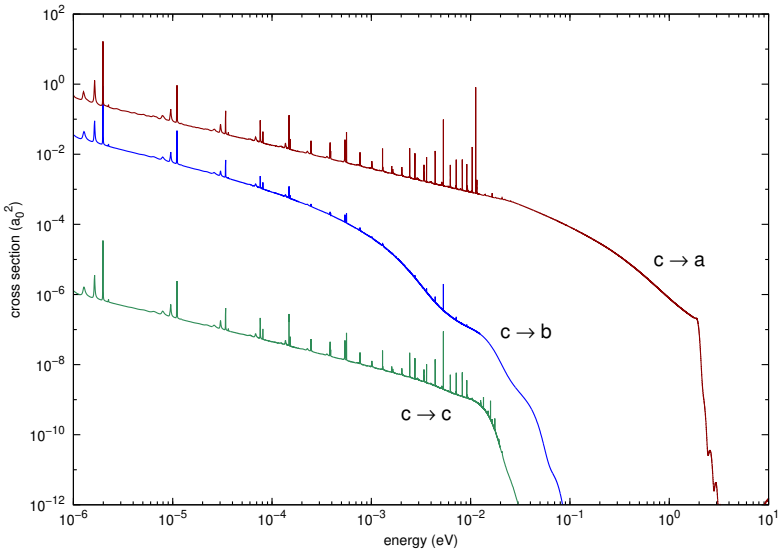

Figure 3: Adapted from Ref. Augustovičová et al. (2015a): Cross sections versus energy for spontaneous ($T_b = 0$ K) radiative association of $LiHe^+$ involving molecular states $a(^3\Sigma^+)$, $b(^3\Sigma^+)$, and $c(^3\Sigma^+)$. Displayed are only the contributions of resonances with widths wider than 0.01 cm^{-1}.

tional states also substantially affects the total cross section. Another considerable impact on increase of $\sigma(E)$ is the number of appropriate symmetry-allowed resonances as such, for which the corresponding Hönl-London coefficients are non-zero, throughout the character of a quasi-bound state wave function $\chi_{J'}(E, R)$. The wave function for a resonant energy picks up amplitude at the barrier and generates then a larger overlap in the well region with a transition dipole (quadrupole) moment function for the transition to a lower-lying level as the integral (3) depicts.

The corresponding rates of formation of the selected molecular ions of astrophysical importance (HeH^+, HeD^+, $LiHe^+$, and He_2^+) were calculated as functions over a wide range of temperatures. Since the rate coefficient can be seen as a Laplace-transform image that smoothens the resonance structure (Eq. 7), the rates on the temperature scale are thus mimicking the cross-section behavior (cf. Fig. 4 and Fig. 5) on the energy scale.

Barred some noteworthy exceptions rates for all studied association processes are generally decreasing with increasing reaction temperatures.

Out of all the presented papers I will to focus in more detail on one, the outcomes of which I consider most interesting. The four processes that were shown in Fig. 4 illustrate a comparison of spontaneous radiative association driven by quadrupole transitions to those driven by dipole transitions. To my best knowledge, the study (Au-

gustovičová et al., 2015a) presents for the first time a direct comparison between molecular formations of homonuclear diatomic ions induced by electric quadrupole transitions with those induced by electric dipole transitions.

Within this work four $^2\Sigma^+$ states of He_2^+ were involved (from the lowest in energy $X(^2\Sigma_u^+)$, $A(^2\Sigma_g^+)$, $B(^2\Sigma_u^+)$, and $D(^2\Sigma_u^+)$), whereby the extra symmetry classification of gerade (g) and ungerade (u), which is available in homonuclear molecules such as H_2^+ and He_2^+, introduces new selection rules that are applied to radiative transitions. The transitions from the initial Σ_u^+ states proceed towards Σ_g^+ states via dipole moment, while Σ_u^+ states are only achievable via quadrupole moment transitions. In principle, the quadrupole transitions conserving $g \leftrightarrow g$ symmetry may be considered, but a shallow potential well of the $A^2\Sigma_g^+$ electronic state supports only a few target rovibrational states, so the corresponding transition moments are expected to be inconsiderable. These processes in the mentioned scheme are labelled as $B \to A$ or $D \to A$ (dipole), and $B \to X$ or $D \to X$ (quadrupole), respectively.

Normally, one expects the cross sections for quadrupole-induced transitions to be at least four orders of magnitude smaller than those for dipole-induced transitions, where the major argument comes from c^5 dependence in contrast to c^3 in the denominator of the respective cross-section formulas (1) and (2). Nevertheless, the combina-

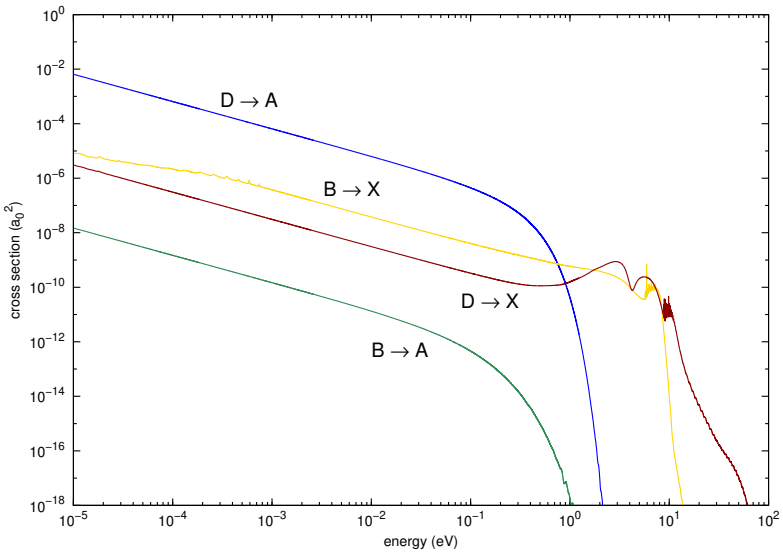

Figure 4: Adapted from Ref. Augustovičová et al. (2015a): Cross sections versus energy for spontaneous ($T_b = 0$ K) radiative association of He_2^+ involving molecular states $D(^2\Sigma_u^+)$, $B(^2\Sigma_u^+)$, $A(^2\Sigma_g^+)$, and $X(^2\Sigma_u^+)$. Transitions labeled $B \to A$ and $D \to A$ are dipole-driven, $B \to X$ and $D \to X$ are quadrupole-driven. Displayed are only the contributions of resonances with widths wider than 0.01 cm^{-1}.

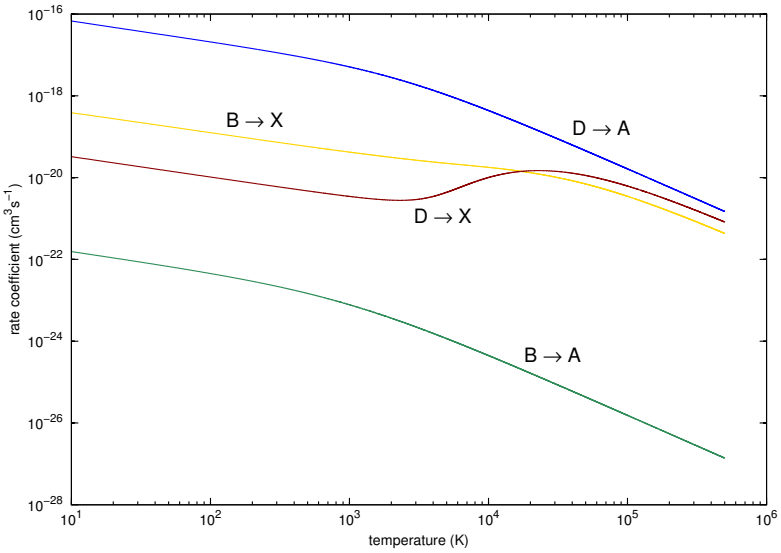

Figure 5: Adapted from Ref. Augustovičová et al. (2015a): Rate coefficients versus temperature for spontaneous ($T_b = 0$ K) radiative association of He_2^+ involving molecular states $D(^2\Sigma_u^+)$, $B(^2\Sigma_u^+)$, $A(^2\Sigma_g^+)$, and $X(^2\Sigma_u^+)$. Transitions labeled $B \to A$ and $D \to A$ are dipole-driven, $B \to X$ and $D \to X$ are quadrupole-driven.

tion of several factors can favorably influence the size of quadrupole-induced cross sections. The factors that play a significant role are: First, the depth of the target potential, thus the number of accessible rovibrational levels supported by this electronic state. Second, the Franck–Condon overlaps between the initial and target state wave functions. Third, the size of the corresponding transition moments (see Fig. 2 in Augustovičová et al., 2015a).

The calculated cross sections and rate coefficients inferred from them are displayed in Figs. 4 and 5 for the four considered processes. Surprisingly, all these aspects give rise to the quadrupole cross sections that are fairly comparable to the dipole ones. A couple of additional reasons can be named which may give a better explanation to this outcome. Mainly, it is the large difference in the numbers of rovibrational bound states in the target X and A states, 409 in X versus 6 in A. Moreover, quadrupole-induced transitions allow for three branches (O, Q, and S) within a band of a molecular spectrum of He_2^+, while dipole-induced transitions offer only two branches (P and R). Their relative strengths are indicated by the Hönl-London factors (4) and (5). These facts result in that the quadrupole-driven radiative association processes $B \to X$ or $D \to X$ have many more (by approximately a factor of 100) summands contributing to the total cross sections. The large difference between the efficiencies of two association reactions induced by electric dipole $D \to A$ and $B \to A$ can be explained through different Franck-Condon conditions as Fig. 4

in Augustovičová et al. (2015a) demonstrates, and through the non-vanishing dipole moment function for large internuclear distances (see Fig. 2 in the same reference).

The radiative association results have been compared to non-radiative inelastic and de-excitation processes treated beyond the Born-Oppenheimer approximation (Belyaev et al., 2014; Belyaev et al., 2015). Studies of non-adiabatic effects performed on different excitation levels of collisional complexes Li^+ + He and Li + He^+ can contribute to a better understanding of primordial and interstellar lithium chemistry, especially when comparing the efficiencies of radiative and non-radiative processes at different temperatures in astrophysical environments.

Quantum non-adiabatic nuclear dynamics takes into account radial non-adiabatic coupling matrix elements between states of the same symmetry of the low-lying $^{1,3}\Sigma^+$ and $^{1,3}\Pi$ states of the $LiHe^+$ ion to determine non-radiative inelastic cross sections and rate coefficients for all partial processes between the scattering channels. In contrast to radiative cross sections, the non-radiative ones generally increase with increasing collision energy (see Figs. 5 and 6 in Belyaev et al., 2015), owing to the fact that dominating partial channels are essentially endothermic. This behavior is reflected in a general increase of

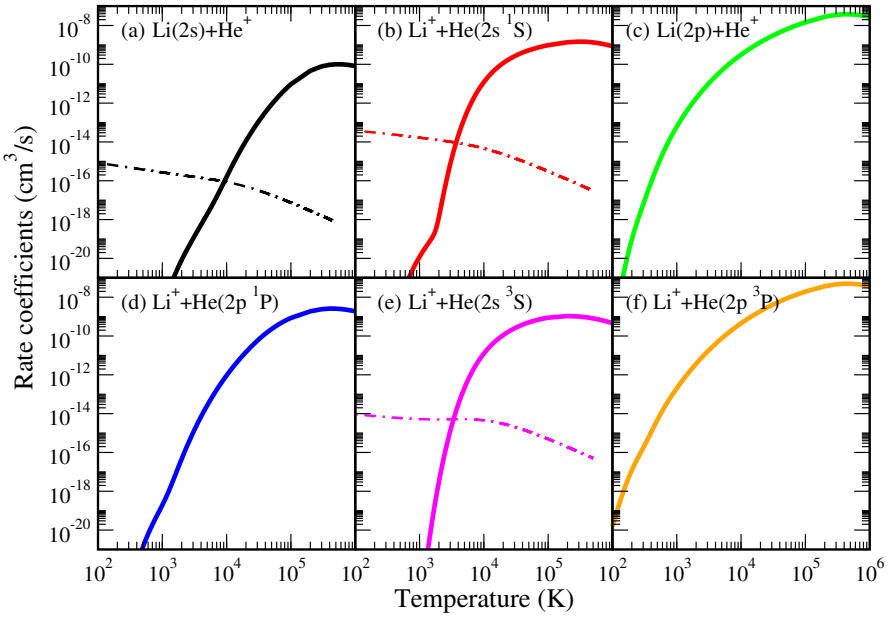

Figure 6: Adapted from Ref. Belyaev et al. (2015): Total rate coefficients for non-radiative (solid lines) and radiative (dot-dashed lines) inelastic processes in lithium–helium ion–atom collisions for different initial channels as a function of temperature. The initial collisional channel is indicated in each panel. The data for radiative depopulation are taken from (Augustovičová et al., 2012; Augustovičová et al., 2014a; Augustovičová et al., 2014b).

the corresponding rate coefficients as a function of temperature (Fig. 3 in Belyaev et al., 2014 and Fig. 7 in Belyaev et al., 2015).

They are compared with available total radiative rate coefficients (Augustovičová et al., 2012; Augustovičová et al., 2014a; Augustovičová et al., 2014b) for the same initial channels. As shown in Fig. 6, whereas the rate coefficients of the non-radiative processes increase rapidly with increasing temperature, the rate coefficients of the radiative processes drop slowly for high temperatures.

The findings evidence that at low temperatures the radiative depopulation in Li^+ + He and Li + He^+ collisions dominates over the non-radiative processes at temperatures up to ~ 9 000 K, while in Li^+ + He(2^3S) or Li^+ + He(2^1S) collisions only up to a critical temperature ~ 3 400 K or ~ 3 700 K, respectively. Thus the latter reactions are expected to have some influence on depopulations of metastable He in high temperature astrophysical environments.

Based on these results, we can summarize that at relatively high temperatures a non-radiative decay (due to non-adiabatic transitions) is expected to be more efficient than a radiative decay for higher-lying excited states. A critical temperature separating radiative and non-radiative reactions needs to be determined in each particular case.

More broadly, it appears that non-radiative and radiative processes apply to different areas in interstellar environments when surveying atomic or molecular astrophysical questions. In particular, non-radiative collision processes can, therefore, be expected to be dominant in stellar atmospheres. On the other hand, the radiative processes are typically the more efficient ones at low temperatures, such as in molecular clouds or in other cold astrophysical environments.

2

SPECTRAL PROBES OF POSSIBLE VARIABILITY OF FUNDAMENTAL CONSTANTS

The two cornerstones of modern physics – Standard Model (SM) of particle physics and General Relativity (GR) theory have been remarkably successful in the description of existing phenomena and prediction of new ones (Patrignani C. et al. (Particle Data Group), 2016). In contrast to their great success, there are major problems inseparably intertwined with these theories. The imbalance of matter and antimatter (Dine and Kusenko, 2003), the existence and properties of the dark matter (Bertone, 2013), the accelerating expansion of the Universe (Perlmutter, 2012) connected with dark energy and the frustrating failure of all attempts to combine physics of Standard Model with gravity are the most glaring examples. Thus, the search for possible physics beyond the Standard Model can have profound impact on our understanding of the nature of Universe and its laws.

The SM considers all fundamental constants as invariable in time and space. Many theories that go beyond GR and SM allow variability of these constants (Uzan, 2011). Most recent studies on variation of fundamental constants focus on dimensionless constants, especially the proton to electron mass ratio μ and the fine structure constant α as their values are not dependent on the chosen system of units of measurement (Safronova et al., 2018).

As the possible space or time variability of μ or α is reflected in the spectra of atoms and molecules that are dependent on these constants, the most accurate tests of their variability in modern era are performed using atomic clocks. The combination of constraints from atomic clock experiments carried out with different species (Godun et al., 2014) gives the following limits to the present day variation of μ and α (Safronova et al., 2018):

$$\frac{\dot{\mu}}{\mu} = (0.2 \pm 1.1) \times 10^{-16}\,\text{year}^{-1},$$
$$\frac{\dot{\alpha}}{\alpha} = (-0.7 \pm 2.1) \times 10^{-17}\,\text{year}^{-1}.$$

Similar values were reported by Huntemann et al. (2014) who analyzed different sets of atomic clock frequencies related to Cs microwave clock.

Molecules possess rich spectra that enable many different types of transitions. In the Born-Oppenheimer approximation the energy (frequency) of the rovibronic transitions depend on μ as

$$E \sim c_{\text{elec}} + c_{\text{vib}}\mu^{-1/2} + c_{\text{rot}}\mu^{-1},$$

where c_{elec}, c_{vib} and c_{elec} are not functions of μ. Hence, the purely vibrational and rotational transitions have sensitivity factors to variation of μ, $K_\mu = -1/2$ and $K_\mu = -1$, respectively. The sensitivity factor describes the relative change of energy (frequency) of given transition due to relative change of the value of the proton to electron mass ratio:

$$\frac{\Delta E}{E_0} = K \frac{\Delta \mu}{\mu_0},$$

where the subscript 0 denotes the present value of transition energy or μ. Additional types of dependences of K on μ arise after inclusion of fine and hyperfine structure, Λ-doubling etc. (Chin et al., 2009).

Pioneering experiments on utilization of molecular clocks for studies of fundamental constants variation were performed by Shelkovnikov et al. (2008) who used Ramsey spectroscopy to probe rovibrational transition in a supersonic beam of SF_6. Theoretical studies by Beloy et al. (2010) and Flambaum and Kozlov (2007) have shown that accidental degeneracies between vibrational and fine structure levels can lead to a substantial enhancement of the sensitivities to variation of both α and μ in many diatomic systems, such as Cl^+, CuS, HfF^+, IrC, and SiBr. An increase of sensitivities on variation of α by 2 to 3 orders of magnitude due to cancellation between the hyperfine and rotational intervals was reported by Flambaum (2006).

Chin and Flambaum (2006), and Gacesa and Côté (2014) proposed to probe the possible variation of fundamental constants using precise measurement of scattering lengths in Bose-Einstein condensate and in photoassociation of ultracold molecules near a Feshbach resonance. An incremental progress was made in laboratory spectroscopic tests on variation of μ for ultracold deuterated ammonia released from an electrostatic trap and recaptured after chosen time (Quintero-Pérez et al., 2014) and for high resolution spectroscopy of methanol and its deuterated isotopologue in a Stark-deflected molecular beam (Jansen et al., 2013). The main aim of the latter studies has been an improvement in precision in reference to the astrophysical searches of μ variation.

While the laboratory studies focus on possible present variation of fundamental constants on a time scale of years, a complementary avenue of research aims to probe their variation in distant past, wherein the time scale is given by the age of the Universe. A distant bright astrophysical light source such as quasar is needed to provide illumination of high-redshift interstellar gas clouds enabling observation of atomic and molecular spectra with an age of up to several billion years. Such spectra can then be compared to the results from the high resolution laboratory experiments.

As the Universe expands, the light from distant objects is redshifted with a cosmological redshift z defined as

$$z = \frac{\lambda_{obs} - \lambda_{lab}}{\lambda_{lab}},$$

where λ_{lab} is the wavelength of the absorbed or emitted radiation and λ_{obs} is the wavelength of the light as observed on Earth. The higher the redshift z the longer the look-back time in the history of the Universe.

Presently the best astrophysical constraint on variation of μ for high redshifts of up to $z = 4.2$ (12.4 billion years) was obtained by Ubachs et al. (2016) from the 10 absorption systems of the H_2 molecule using UV transitions in the Lyman and Weber bands that are redshifted to the visible spectrum with z in the range of 2.0 to 4.2. Although the maximum sensitivity coefficient of these transitions was only $\Delta K_\mu \approx 0.06$ (Kozlov and Levshakov, 2013), the limit on temporal variation of μ set by the study of Ubachs et al. (2016) was

$$\left|\frac{\Delta\mu}{\mu}\right| = \left|\frac{\mu_{obs} - \mu_{lab}}{\mu_{lab}}\right| \leqslant 5 \times 10^{-6}\ (3\sigma), \tag{12}$$

where μ_{obs} was inferred from the astrophysical observations and corresponds to the value of μ in distant past and μ_{lab} is the current value of μ obtained from contemporary laboratory studies.

The most stringent constraint on possible time variation of μ, albeit for lower redshifts ($z = 0.89$), was set by Bagdonaite et al. (2013a) and Bagdonaite et al. (2013b) using several absorption lines of methanol molecule observed towards PKS 1830-211. Methanol is present in sufficient densities in many interstellar environments and has relatively high sensitivity coefficients with $\Delta K_\mu \approx 60$ (Kozlov and Levshakov, 2013). The obtained limit of $\Delta\mu/\mu = (-1 \pm 0.8_{stat} \pm 1.0_{sys}) \times 10^{-7}$ (Bagdonaite et al., 2013a) gives assuming linear change of μ with time $\dot{\mu}/\mu = 2 \times 10^{-17}\text{year}^{-1}$. This is more strict than the corresponding limit inferred from atomic clocks (Huntemann et al., 2014; Godun et al., 2014).

Other astrophysical systems were considered for studies of temporal variation of μ. The transitions of ammonia isotopologues (especially inverse transitions) promise to potentially improve limits on μ variation (Augustovičová et al., 2016; Špirko, 2014; Flambaum and Kozlov, 2007; Murphy et al., 2008; Henkel, C. et al., 2009; Kanekar, 2011) as ammonia is ubiquitous in the interstellar medium and possess several transitions with very high sensitivities (Jansen et al., 2014 reported sensitivity coefficient of -938, while Špirko (2014) and Owens et al. (2016) found a transition with $K_\mu = -16\,737.52$). Rather high sensitivity coefficients were also reported for H_3O^+ and D_3O^+ molecular ions (Owens et al., 2015) and for the phosphine molecule (Owens et al., 2018). Unfortunately, in all these cases the highest sensitivity coefficients correspond to forbidden transitions and therefore the

particular lines are very weak. Recently, primordial diatomic cations H_2^+, D_2^+ and He_2^+ were suggested as feasible probes of μ variation at very high redshifts owing to the high sensitivity coefficients of their microwave rovibronic transitions (Augustovičová et al., 2014c). The search for possible spatial or temporal variation of fundamental constants is also substantially facilitated by rapid evolution of astronomical detection techniques such as VLBI, ALMA and FAST telescope (Martí-Vidal, I. et al., 2013).

2.1 RESULTS FOR SELECTED SYSTEMS

The sensitivity coefficient K_μ for transition between two states with energies E_u (upper state) and E_l (lower state) can be described by a linear proportionality (Jansen et al., 2014)

$$K_\mu \equiv K_{u,l} = \frac{\mu}{E_u - E_l}\left(\frac{dE_u}{d\mu} - \frac{dE_l}{d\mu}\right). \tag{13}$$

The frequency shift ($\Delta\nu = \nu_{obs} - \nu_0$) of a given transition due to a temporal variation of μ (where $\Delta\mu = \mu_{obs} - \mu_0$) depends on K_μ through the expression

$$\Delta\nu = \nu_0 K_\mu \frac{\Delta\mu}{\mu_0} = (E_u - E_l)K_\mu \frac{\Delta\mu}{\mu_0} = S_\mu \frac{\Delta\mu}{\mu_0}. \tag{14}$$

The subscript 0 denotes present day values of μ or ν, while those inferred from observations of distant objects are labelled by the subscript "obs".

When choosing promising systems for astrophysical studies of possible μ variation several considerations have to be taken into account. First, the sensitivity coefficient itself of a given transitions. Several transitions with high absolute value and different sign of K_μ are desirable. Second, the intensity of the particular transitions as often the highest K_μ are related to forbidden transitions with very low Einstein A coefficients. Third, the abundance of the studied molecular specie in the Universe and especially at high redshifts - only such species whose laboratory spectra can be compared to the astrophysical observations are suitable candidates.

The publication (Augustovičová et al., 2014c) predicts the sensitivity coefficients and various spectral characteristics of ro-vibrational transitions between the lowest lying electronic states of H_2^+, D_2^+ and He_2^+ cations that are supposed to had played a key role in the chemical evolution of the early Universe and as such can be expected to be observable at very high redshifts. It is necessary to point out that the studied cations H_2^+, D_2^+ and He_2^+ have not yet been detected in the extraterrestrial environments and their very detection is considered a daunting task. On the bright side, the characteristic time scale for H_2^+ destruction in reactive collisions with atomic or molecular hydrogen is much longer than the radiative lifetimes (up to 1000 s) of the

H_2^+ states whose microwave transitions were covered in the presented study with details in Ref. (Augustovičová et al., 2014c).

To obtain sensitivity coefficient K_μ for a spectral transition between an upper and lower state with their energies, E_u and E_l, respectively, we adopted an indirect approach, in which we relied on extensive high-level ab initio calculations that were subsequently morphed by fitting to extremely accurate experimental data. The calculations themselves for H_2^+, D_2^+ and He_2^+ were based on direct non-linear fit of the spectroscopic data in microwave range (e.g. Carrington, 1996) and of the available theoretical rovibrational energies to obtain reliable potential energy curves. To respect the fact that the available experimental data are rather scarce, we performed our fitting in the framework of the Jenč's Reduced Potential Curve (RPC) approach (Jenč, 1983; Jenč et al., 1993). The RPC method provides a suitable tool for a quantitative morphing of accurate ab initio potential energy curves in terms of only a small number of morphing parameters (Patkowski et al., 2009; Špirko, 2016). Moreover, the accuracy of resulting potentials can be enhanced by incorporating ab initio calculated coefficients to the fits when available.

In addition, the approach of computing sensitivity coefficients for a molecular system made use of an effective Hamiltonian model to probe how the parameters of this model depend on μ. The required numerical derivatives, $dE_x/d\mu$, for $x = u, l$, were obtained from the calculated dependences of particular energies on μ. The variational approach is advantageous in that along with sensitivity coefficients, reliable theoretical transition frequencies can be predicted if no experimental data are available, and it also allows a comprehensive

Table 1: Adapted from Ref. Augustovičová et al. (2014c): The $A^2\Sigma_u^+ \leftrightarrow X^2\Sigma_g^+$ microwave transitions of H_2^+ (frequencies ν in MHz, line strengths S in D^2, Einstein coefficients A in s^{-1}). Experimental data from Ref. Carrington et al. (1995).

ν', N'	ν'', N''	ν_{fit}	ν_{exp}	S	A	T
			$A \to X$			
0, 0	18, 1	514956.6		3.073	2.038×10^{-01}	31.669
0, 1	18, 0	645722.3		2.484	1.083×10^{-01}	26.982
0, 1	18, 2	352014.8		7.493	5.293×10^{-02}	39.683
0, 2	18, 1	593778.1		4.452	9.055×10^{-02}	27.400
0, 2	18, 3	156614.7	156633	15.406	5.751×10^{-03}	65.568
			$X \to A$			
19, 0	0, 1	52907.5	52895	8.884	6.400×10^{-04}	-17.594
19, 1	0, 0	96431.6	96432	5.268	7.659×10^{-04}	-5.739
19, 1	0, 2	17610.2	17610	24.113	2.135×10^{-05}	-29.230

treatment of a molecule to be undertaken. For all transitions analyzed Einstein A coefficients and line strengths S have been calculated to guide future laboratory and astronomical observations using theoretical concepts described in Section 1.1. The values of the calculated sensitivity coefficients are comparable to their 'record-breaking' methanol counterparts (see Table 1 and the supplemental material to Ref. Augustovičová et al., 2014c for the complete list of studied transitions, their sensitivities and other spectral parameters). The largest absolute value of K_μ obtained in this study, $K_\mu = -407$, involved the $(\nu_A = 0, N_A = 3 \leftarrow \nu_X = 26, N_X = 4)$ transition of D_2^+ molecular ion. The fact, that the resulting sensitivity coefficients were of both signs allowing simple analysis without need for reference molecules coupled with the relatively large line strengths of the studied transitions, hints that H_2^+ (and to a lesser extend also D_2^+ and He_2^+) could be a promising candidate for astrophysical tests of μ variation at high redshifts.

The theoretical approach utilized in the above mentioned study of primordial cations H_2^+, D_2^+ and He_2^+ (Augustovičová et al., 2014c) was refined in my subsequent study (Augustovičová et al., 2016) focused on hyperfine structure of rotational-inverse $(\nu_2 = 0^+, 0^-, 1^+, 1^-)$ states of ammonia isotopomers $^{14}NH_3$ and $^{15}NH_3$ by addition of efficient roinverse hyperfine functions. These functions were obtained by simultaneous fitting of available measured transitions using ef-

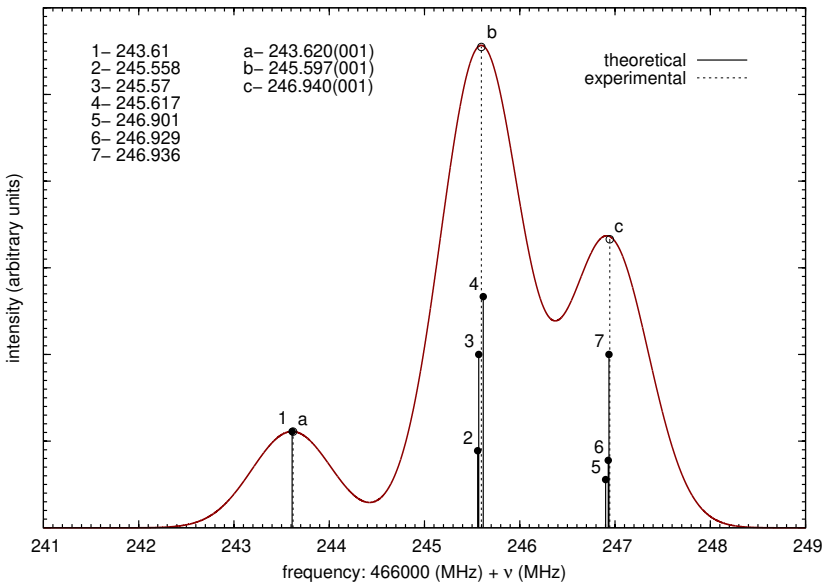

Figure 7: Adapted from Ref. Augustovičová et al. (2016): Theoretical ammonia $^{14}NH_3$ $\nu_2 = 1, (J, K) = (1, 0)^+ \rightarrow (0, 0)^-$ spectrum vs. saturation dip position lines of the hyperfine components from (Belov et al., 1998) at temperature 150 K. Frequencies are given in MHz relative to the value of 466,000 MHz.

fective Hamiltonian within the non-rigid inverter theory. The results obtained with the inclusion of only a small number of mass independent fit parameters allowed to provide reliable predictions of hyperfine interactions for a large number of so far unobserved transitions involving roinverse states of ammonia isotopomers as well as critical revision of fits based on mass and state dependent spectroscopic constants.

Precise determination of the hyperfine-structure parameters allows to account for energy level patterns imprinted in the Doppler profile of ro-inversion transitions (e.g. see Figs. 7 and 8), and hence for explanation of physical characteristics that are dependent on these patterns - for example, an accurate determination of Boltzmann constant by Doppler spectroscopy (Lemarchand et al., 2011) or modeling of the laser-induced population transfers. In particular, the published predictions can be used to derive the true centers of astronomical line bands that come to the forefront of fundamental physics and seem promising for critical testing of the cosmological variability of μ.

Ammonia is abundant in a variety of interstellar environments and has been detected not only in our Galaxy but also in very distant astronomical objects with redshifts $z \sim 0.685$ and $z \sim 0.886$ (Henkel, C. et al., 2005; Henkel, C. et al., 2008) currently providing spectral lines that allow a critical limitation regarding changes in ration of proton mass to electron mass on cosmological timescales.

As documented in the case of ammonia molecule, the dependence of sensitivity coefficient K_μ on the reciprocal value of the transition

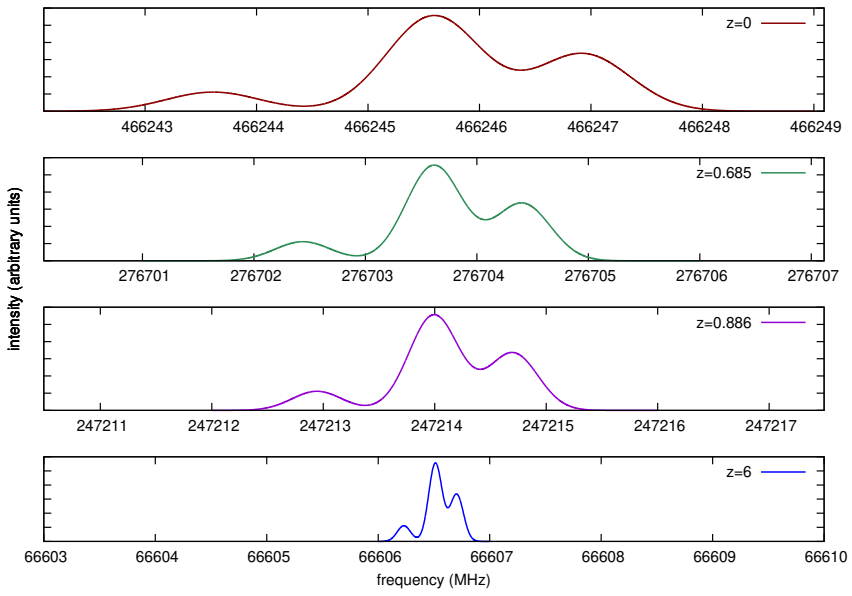

Figure 8: Theoretical ammonia $^{14}NH_3$ $\nu_2 = 1, (J, K) = (1, 0)^+ \rightarrow (0, 0)^-$ Doppler spectra lineshapes for various redshifts at temperature 150 K.

frequency can lead to its strong enhancement in case of accidental degeneracies of the corresponding energy levels. Thus by tuning the energy levels degeneracy, such as in the Zeeman-tuned level-crossing spectroscopy (Cahn et al., 2014), a dramatic increase of the value of K_μ can be achieved. The magnetic field, detected in almost every astrophysical object in the Universe, and believed to play an important role in the dynamics of the interstellar medium (Crutcher, 1999; Crutcher, 2012), could be utilized not only for significant enhancement of the sensitivities but also for reduction of the Doppler broadening of the studied transitions that often hinders precise astrophysical observations.

The hydroxyl radical (OH) was chosen as a model system for the study on the effects of the magnetic fields on the mass sensitivities of the spectral transitions of molecular radicals exhibiting Zeeman splittings (Augustovičová and Špirko, 2020). OH is present in large quantities in many astrophysical objects including those with very high redshifts. Recently the study by Spilker et al. (2018) reported observation of OH spectra towards SPT2319-55 with $z \sim 5.3$ corresponding to the look back time of 12 billion years. Moreover, the energy level pattern of the rotational ground state is especially suitable for Zeeman tuning of relative distance of particular hyperfine energy levels.

The hydroxyl radical in its electronic ground state X posses a $^2\Pi$ configuration. Each rotational level, labelled by quantum number J consists of a Λ doublet with states described by $+$ and $-$ parities (and labelled here by the usual spectroscopic notation e and f, respectively). Under the influence of the magnetic field each of these components splits into several sublevels (see upper panel of Fig. 9 and a detailed analysis in the Appendix A), and as a result, the Zeeman level patterns corresponding to the e and f parity topologically almost coincide.

The Zeeman energy and mass sensitivity patterns of the rotational states of the paramagnetic OH radical in its ground electronic state were probed using a complete molecular Hamiltonian. The Zeeman energy splittings exhibit nearly coinciding magnetic dependences with their corresponding 'reduced' mass sensitivities. For the low magnetic fields that are too weak to compete with the hyperfine interactions rather nonlinear shapes of the Zeeman spectra occur, while for the fields dominating the hyperfine interactions the Zeeman effect is nearly linear with the change of B. As the slopes of the individual split Zeeman lines acquire positive and negative values, the energy levels in the imposed magnetic field undergo level-crossings.

The decrease in the transition frequencies related to these crossovers provides a dramatic enhancement of the mass sensitivity coefficients K_μ of the involved transitions and also a substantial reduction of their spectral line broadenings. The intensities of $e \leftrightarrow e$ and $f \leftrightarrow f$ magnetic dipole allowed transitions are diminished to zero

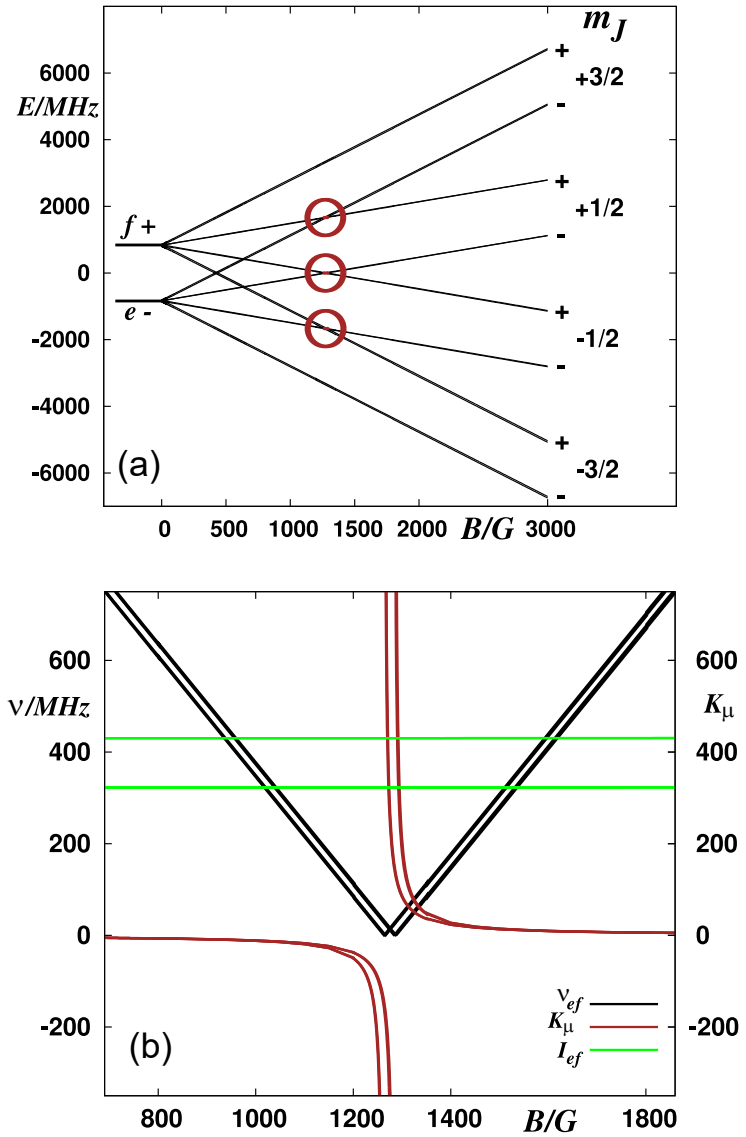

Figure 9: Adapted from Ref. Augustovičová and Špirko (2020): Energy level patterns E [panel (a)], allowed transition frequencies ν, mass sensitivities K_μ and relative intensities I (in arbitrary units) [panel (b)] of ^{16}OH in its $J = 3/2$ rotational state. Colored circles label level-crossing states supporting allowed transitions [colored curves in panel (b)].

as the values of the corresponding frequencies are reduced. Therefore, their possible use in astrophysical analysis of cosmological constant variability is limited. On the other hand, the intensities of the $e \leftrightarrow f$ electric dipole allowed transitions are almost constant in the imposed field as shown in the lower panel of Fig. 9. Moreover, these transitions are much stronger than their magnetic counterparts and thus they appear to be very promising astronomical probes for the cosmological variability of the proton-to electron mass ratio.

Paramagnetic spectrum analysis obtained in the presence of extremely strong magnetic fields seems to be particularly interesting, because the absolute sensitivity factors S_μ of the corresponding transitions increase monotonously with the field strength. It therefore seems conceivable that these analyzes could improve the current limit of the temporal variation of μ.

However, it should be emphasized that current results were obtained using constant molecular g-factors with total neglect of higher order diamagnetic contributions. The diamagnetic contributions are quadratic in B and their role in the case of extremely strong magnetic fields could become important.

3

TOWARD ABSOLUTE ZERO TEMPERATURE

Cooling atoms to ultralow temperatures has offered new insights into fundamental physics (e.g. Bose-Einstein condensate, superfluidity, degenerated Fermi gases), precision measurement, quantum information processing and quantum optics. Ultracold physics as well as its applications have undergone a remarkable progress thanks especially to very recent experimental developments such as molecular laser cooling (Shuman et al., 2010; Barry et al., 2014; Yeo et al., 2015; Kozyryev et al., 2016; Chae et al., 2017) and buffer-gas-loaded beams (Hutzler et al., 2012). With sophisticated cooling techniques – resulting in several Nobel Prizes (Chu, Cohen-Tannoudji, Phillips, Haroche, Wineland) – applied to molecules, whose implementation has been more challenging due to the complexity of molecular structures, the longstanding goal of accurately controlling molecular degrees of freedom and the resulting interaction processes seems to be finally within reach. Further insight on how molecules interact can in turn lead to more precise control of reaction chemistry (Bohn et al., 2017).

In particular, the technology of laser cooling molecules has paved the way for the production of a long list of truly ultracold molecular species, with temperatures reaching microKelvin rather than the milliKelvin scale (McCarron et al., 2018a). At such low temperatures the molecules can be confined in magnetic (Williams et al., 2018; McCarron et al., 2018b) or optical dipole traps (Anderegg et al., 2018; Cheuk et al., 2018), it is possible to prepare them in individual quantum states, their collisions are governed by individual partial waves and are strongly influenced by laboratory electric and magnetic fields (Krems, 2019). However this technique is at present limited to a particular subset of molecules. In comparison, although still limited to sample temperatures of hundreds of mK, the buffer-gas-loaded beams prove to be very versatile sources.

One of the methods utilized to reach the ultracold regime for a number of chemically relevant species, for which additional cooling is desirable, is the process known as evaporative cooling. Evaporative cooling is a continuous process of decreasing the average energy of a system of trapped particles. This is maintained by flying of atoms in the high-energy tail of Maxwell-Boltzmann distribution away and then by allowing the rest to rethermalize at a lower temperature. However, the cooling efficiency is subject to repopulation of the thermal distribution tail by collisions which requires a relatively high elastic collision rate and initially a high number density of the ensemble related to rethermalization rate (Bohn and Jin, 2014). Yet fulfill-

ment of the rethermalization condition is slowed down by chemical, or primarily, by inelastic collisions during which one or both collision partners change their internal state. The internal state conversion manifests itself in a spin-flip transition or parity change, leading to associated particle losses. Moreover, the inelastic collisions are typically exothermic which leads to additional heating of the trapped atoms or molecules. The technique works well for alkali atoms, where it was noted long ago that the ratio of elastic to inelastic collision rates should exceed ~ 100 for evaporation to be effective (Monroe et al., 1993). For molecules, it has been somewhat difficult to achieve this ratio, because they possess rotational structure and dipole moments ensuing in a substantial number of energy levels, in which they end up after collision. Thus the extension of the evaporative cooling method to molecules, as a secondary cooling process, is not straightforward and has not yet been clearly demonstrated (with a possible exception of OH radical).

A ground state of a polar molecule tends to align dipole moments parallel to the field, known as a high-field seeker. But this state is not trappable because of Earnshaw's theorem. Hence, a desire for finding a configuration with local minimum of the field vector modulus with the purpose of confining cold atoms or molecules in the low-field-seeking states has led experimentalists to design various trapping arrangements employing static or time-varying inhomogeneous fields, such as TOP trap, Ioffe-Pritchard trap, Paul RF trap etc (Ketterle and Druten, 1996; Pérez-Ríos and Sanz, 2013).

It is necessary to point out that for certain ultracold collisions, the scattering rates and their dependences on external fields are determined by physics occurring on scales larger than the range given by the exchange potentials between the collision partners, i. e. when the molecules are far apart. A molecule in a weak-electric-field seeking state can experience torques due to this long range forces and ends up in a strong-field seeking state after collision resulting in losses of trapped particles. One of the advantages of laser-cooled molecules is that they can be optically trapped in strong-field-seeking states being thus more resistant to such state-changing collisions.

In this regard, understanding collision cross sections and their response to applied electromagnetic fields is vital for controlling collisions, which could allow for experimental observation of predicted quantum mechanical effects applicable, e.g. in quantum simulation and computation.

3.1 RESULTS OF ULTRACOLD DIPOLAR MOLECULAR COLLISIONS

In this section I will briefly describe the structure of the studied molecules, the theoretical approach of molecular scattering and present outcomes. In the absence of an applied field, the effective

Hamiltonian for the fine and hyperfine structure of a free diatomic radical in its ground $^2\Pi$ state includes the spin-orbit interaction, rotational energy of the molecule in the treatment of the rigid body, spin-rotation interaction, Λ-doubling terms, and nuclear hyperfine interaction. The theoretical analysis of the NO spectra is similar to that already described for OH radical, but with features arising from different nuclear spin (^{14}N nucleus has spin $I = 1$, the spin of the hydrogen nucleus is $1/2$). Therefore, we can utilize most of the matrix elements derived earlier for OH in Chapter 2 and Appendix A. Components of Λ-doubling are $|\Omega| = 1/2$ and $|\Omega| = 3/2$, both doubly degenerate, of which $^2\Pi_{1/2}$ is the lower-lying state because the spin–orbit coupling constant (for the ground vibrational state) is positive $A = 123.146\ \mathrm{cm}^{-1}$ (Varberg et al., 1999), unlike that of OH, SH or LiO. As indicated in Appendix A we work in a Hund's case (a) basis while the basis functions are of the form

$$|\eta, |\Omega|, (J, I), F, M_F; p\rangle \tag{15}$$

in the hyperfine-coupled basis set. Here η is a general index which represents all other considered quantum numbers and p labels parity.

The list of laser-coolable diatomic species has been recently extended to include classes of polyatomic molecules that are expected to be amenable based on Franck-Condon factors calculations (Isaev and Berger, 2016). Soon after, experimental success in Sisyphus laser cooling of the polyatomic molecules SrOH and YbOH has been reported (Kozyryev et al., 2017; Augenbraun et al., 2020). Augustovičová and Bohn (2019) extended cold collision theory of linear polyatomic molecules, treating ^{40}Ca^{16}OH molecules colliding with each other.

In comparison to laser cooled diatomic molecules, alkaline earth monohydroxide radicals, including CaOH, possess more complicated structure. It has three vibrational modes: a symmetric stretch ν_1, an antisymmetric stretch ν_3, and doubly degenerate bending vibrations ν_2 without a direct analog in diatomics. Additionally, an effect of molecular rotations and vibrations on the electronic spectra of linear molecular species in degenerate electronic states ($\Lambda \neq 0$), the Renner-Teller effect, which is missing in diatomic molecules, further complicates molecular structure. For optical trapping purposes we have focused on the specific state, the lowest bending excitation with $v_2^{|l|} = 1$ of the ground electronic $X\,^2\Sigma^+$ state. This is because it is the lowest-lying state with a doublet and therefore can be easily polarized in a small electric field. The superscript l next to the vibrational quantum number v_2 labels the projection of the vibrational angular momentum on the molecular axis and takes values of $l = -v_2, -v_2+2, \ldots, v_2$. The appropriate hyperfine-coupled case (b) basis set is

$$|X\,(0, 1^{|l|=1}, 0);\ [(N, S)J, I]\,F, M_F; p\rangle \tag{16}$$

of definite parity $(-1)^{N-l}$ and the spin $I = 1/2$ is of the hydrogen atom. The matrix elements of the effective Hamiltonian that includes vibrational and rotational energies, the spin-rotation coupling, the l-type doubling, and the hyperfine interaction are given in Augustovičová and Bohn (2019).

Polar molecules are susceptible to external electromagnetic fields via their electric and magnetic moments. In the case of both considered molecules, NO and CaOH, a magnetic field is less relevant as the molecular magnetic moment due to the electron's orbital motion and spin is insignificant. The Stark Hamiltonian for the molecular dipole – electric field interaction is given by $H_S = -\mathbf{d}_s \cdot \mathcal{E}$, where direction of the homogenous electric field vector $\mathcal{E}$ coincides with the space-fixed Z-axis. Fig. 10 demonstates the electric-field dependence of the $(0, 1^1, 0)$, $N = 1$ levels of CaOH.

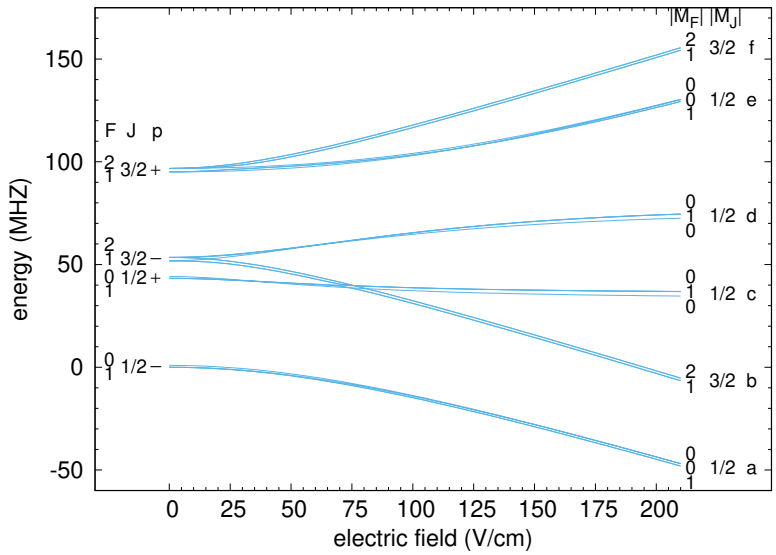

Figure 10: Adapted from Ref. Augustovičová and Bohn (2019): Stark effect in the $(0, 1^{|l|=1}, 0)$, $N = 1$ state of CaOH. At zero field, the states are labeled by the total electron-plus-rotation angular momentum J, the total spin F, and the parity p; at larger electric field the states are labeled by the projections M_J and M_F of these angular momenta along the field axis. Each line is doubly degenerate in lM_F. As a shorthand, the fine structure manifold at high field are labeled by the indices $a - f$.

At ultralow collision energies, the molecular dynamics is dominated by the long-range forces. This includes a R^{-6} van der Waals

interaction, a centrifugal potential and electric dipole-dipole interaction between the two molecules

$$V_{dd}(\mathbf{R}) = \frac{1}{4\pi\varepsilon_0}\frac{\mathbf{d}_1\cdot\mathbf{d}_2 - 3\,(\hat{R}\cdot\mathbf{d}_1)(\hat{R}\cdot\mathbf{d}_2)}{R^3}$$
$$= -\frac{\sqrt{30}d^2}{4\pi\varepsilon_0 R^3}\sum_{q,q_1,q_2}\begin{pmatrix} 2 & 1 & 1 \\ q & -q_1 & -q_2 \end{pmatrix} C_{2-q}(\theta\phi)C_{1q_1}C_{1q_2},$$

where the first-rank tensors as reduced spherical harmonics are functions of Euler angles giving orientation of molecular dipole vectors $\mathbf{d}_1, \mathbf{d}_2$, and $\mathbf{R} = (R, \theta, \phi)$ is the intermolecular vector. The matrix elements of the dipolar V_{dd} operator are evaluated in the two-molecule basis

$$|F_1, M_{F_1}; p_1\rangle|F_2, M_{F_2}; p_2\rangle|LM_L\rangle_S, \tag{17}$$

where the individual kets in the direct product space are one-molecule functions (15) or (16) depending on the molecular species, $|LM_L\rangle$ is a partial wave state satisfying the conservation of the total angular momentum projection on the Z-axis, and the subscript S denotes a symmetrized combination of two identical particles, fermions in the case of NO and bosons as for CaOH molecules.

The exact coupled-channel calculations for molecule-molecule scattering was performed employing the log-derivative propagator method (Johnson, 1973). Cross sections as functions of collision energy were computed from the S-matrix elements for processes in which both molecules remain unchanged (elastic) or at least one molecule converts its internal state to another (inelastic). The scattering rate coefficients K were then defined as $v_i\sigma$, where v_i is the incident collision velocity and σ is the collision cross section.

Evaporative cooling is not impossible to achieve for molecular radicals, as it was actually demonstrated in OH (Stuhl et al., 2012); the possibility of evaporative cooling was scarcely probed for only few other molecular species, partly due to technological limitations for experiments. Recently, I have investigated the situation for the $^2\Pi_{1/2}$ and $^2\Pi_{3/2}$ states of the important atmospheric radical NO (Augustovičová and Bohn, 2017; Augustovičová and Bohn, 2018b), which can be prepared for ultracold experiments by means of Stark decelerator (Vogels et al., 2015) or by other means (Bichsel et al., 2007; Elioff et al., 2003). Therefore, it was deemed to be worthwhile to study whether the ratio between elastic and inelastic collisional rates can be altered by an external electric (or magnetic) field. Example of the dependence of calculated elastic and inelastic rate coefficients for collision energy of 100 mK on electric field is plotted in Fig. 11. The NO molecules in this case are in the states with quantum numbers either $|F, M, p\rangle = |3/2, 1/2; +\rangle$ or $|3/2, 3/2, +\rangle$ before collisions.

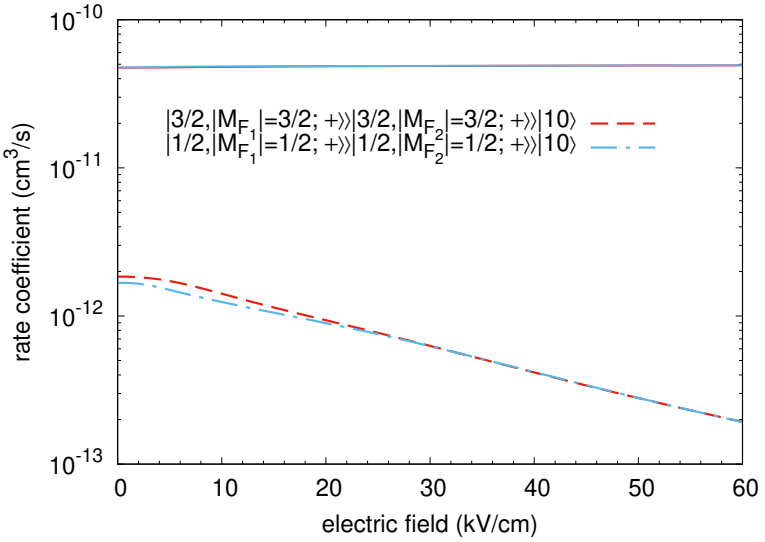

Figure 11: Adapted from Ref. Augustovičová and Bohn (2017): Rate coefficients for elastic (solid curves) and inelastic (dashed curves) scattering as a function of the electric field for the two incident channels $|F = 1/2, |M_{F_1}| = 1/2; +\rangle\rangle|F = 1/2, |M_{F_2}| = 1/2; +\rangle\rangle|L = 1, M_L = 0\rangle_S$ and $|F = 3/2, |M_{F_1}| = 3/2; +\rangle\rangle|F = 3/2, |M_{F_2}| = 3/2; +\rangle\rangle|L = 1, M_L = 0\rangle_S$ of NO molecules. The collision energy is fixed at the value $E_c = 100$ mK.

At all values of electric field the elastic rate coefficients remain high and constant, due to generically strong scattering of polarized dipoles. The elastic rate actually far exceeds the inelastic rate for low electric fields but their ratio is insufficient for the figure of merit of evaporation. After a threshold field of hundreds of V/cm, a new effect appears, namely, the value of the inelastic rate coefficients decrease with increasing electric field. Nevertheless, the suppression effect would require fields as large as 40 kV/cm to exceed 100 for the ratio of elastic to inelastic scattering, which is probably unrealistically high field in electrostatic traps as currently built.

The reasons behind this suppression of inelastic collisional rate coefficient at high electric fields are described in detail in (Augustovičová and Bohn, 2017; Augustovičová and Bohn, 2018b). A qualitative explanation of this high field dependence can be seen if the inelastic scattering of NO molecules is treated using Born approximation. In the field regime where the molecules are fully polarized the losses are controlled by the energy between incident and final thresholds released in the collision. As this energy gap gets larger with electric field the ultracold inelastic rate should scale as $\mathcal{E}^{-1/2}$. Another cause of suppression is due to the matrix elements of the dipole-dipole coupling V_{dd} in the dressed states of the molecules that depend strongly on electric field; the most probable inelastic process is the one that changes the sum of total angular momentum projec-

tion for both collision species by one while the molecular state parities p_1, p_2 are preferred to be changed.

The found non-trivial field dependence of the inelastic collisional rate coefficient is surprising given the conclusions of related studies (see e.g., Avdeenkov and Bohn, 2002 or Fig. 5 in Augustovičová and Bohn, 2019), so it is worth contemplating its applicability to other polar molecules. For the reasons outlined earlier in this section mainly in the context of designing efficient laser cooling schemes I have focused on ultracold collisions of CaOH with the main goal to investigate the possibility of evaporative cooling in an appropriate state. To this end, molecules in the b fine structure manifolds (in the notation of Fig. 10) were considered. Fig. 12 presents rate coefficients as a function of field strength at two different collision energies, 1 mK and 1 μK, for incident channel built of the spin-stretched $|b, l = 1; M_F = 2\rangle$ molecular states.

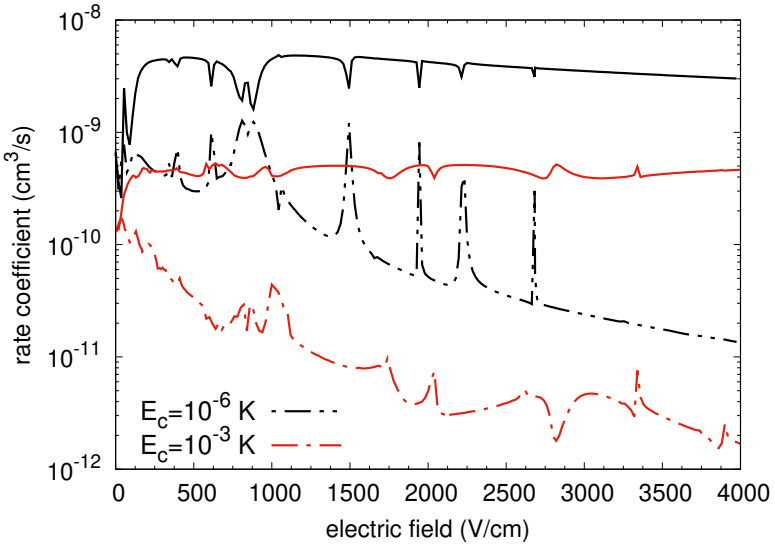

Figure 12: Adapted from Ref. Augustovičová and Bohn (2019): Rate coefficients for elastic (solid curves) and inelastic (dashed curves) scattering as a function of electric field. The collision is initiated in the states $|b, l = 1; M_F = 2\rangle$ of CaOH molecules at two different collision energies $E_c = 1\mu K$ (black lines) and $E_c = 1$ mK (red lines).

In contrast to the case of NO molecular scattering the field dependence of inelastic collision rates is much more favorable for CaOH. Not only do collisions feature an overall decreasing trend of loss rates with applied electric field at both energies but they also decay faster, and thus the ratio of elastic to inelastic collisions above 10^2, as a rule of thumb, occurs at experimentally reasonable field strengths. The obtained results indicate that for $E_c = 1$ mK such a field is $\mathcal{E} \sim 3500$ V/cm while for $E_c = 1$ μK the critical field is $\mathcal{E} \sim 2500$ V/cm.

The cause of this suppression of inelastic scattering is described in detail in Augustovičová and Bohn (2019), which estimates transition amplitudes in the Born approximation as was found useful in the explanation of the phenomenon found out for NO collisions. In a nutshell, for a large field, say $\mathcal{E} > 200$ V/cm, the dominant contribution to the total state-changing rate coefficient is from the final channel $|b, l = 1; M_F = 2\rangle|a, l = 1; M_F = 1\rangle|L = 2, M_L = 1\rangle$. The R-independent off-diagonal matrix elements $|C_{i,f}|$ of dipole-dipole interaction V_{dd} rapidly vanish with an increasing electric field as $\gamma/(d\mathcal{E} + \gamma)$, where γ is the spin-rotation constant, and the contribution to the total inelastic rate from such final channel decreases much faster, with the square of $C_{i,f}$. The weak coupling between a b-level and an a-level is related to the matrix elements of the Stark Hamiltonian H_S diagonal in M_N (the projection of the rotational angular momentum N along the field axis) perturbed by coupling terms that trigger the splitting of $M_N = 1$ energy levels due to spin-rotation interaction.

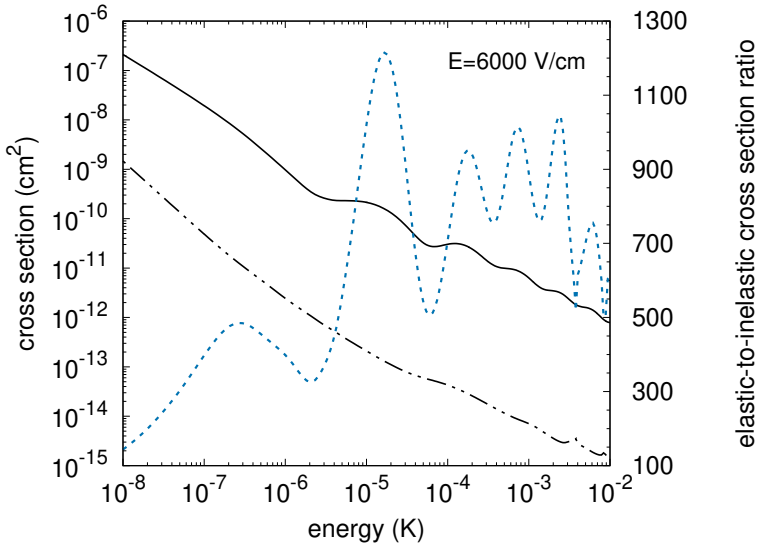

Figure 13: Adapted from Ref. Augustovičová and Bohn (2019): Cross sections for elastic (solid curve), inelastic (dash-dotted curve) scattering, and their ratio (dotted curve, right-hand axis) as a function of collision energy. The collision is initiated in the states $|b, l = 1, M_F = 2\rangle$ of CaOH molecules at an electric field of $\mathcal{E} = 6000$ V/cm.

It turns out that optically trapped CaOH molecules exposed to an electric field in the fine b state with $M_F = 2$ appear be a suitable candidate for viability of further cooling down to ultracold domain driven by elastic collisions and evaporation. This optimistic message is supported by Fig. 13 showing the calculated elastic σ_{el} versus inelastic σ_{inel} cross sections (and their ratio) versus collision energy at a fixed value of electric field, $\mathcal{E} = 6000$ V/cm. On the whole studied range, from 10 mK down to 10 nK, the ratio $\sigma_{el}/\sigma_{inel}$ exceeds 2

orders of magnitude with a maximum at energies $\sim 10\,\mu K$ evidencing that the ratio can be even 1000 or larger. This ratio plummets to zero with lower collision energies because of the Wigner threshold laws that govern elastic cross section to approach a constant while the state-changing cross section varies as $E_c^{-1/2}$.

In addition, it is predicted that by selecting molecules in the f-state, collisions can create newly described “field-linked" dimers by ramping the electric field across the resonance. Upon formation, the long range field-linked states can hold a molecular dimer $(CaOH)_2$ in the lifetime of μs order (Augustovičová and Bohn, 2019), providing another degree of control by giving the experimenter time to further manipulate the molecules. Such ability could provide excellent tools for studying the reaction chemistry and molecular dynamics.

4

QUANTUM CHAOS EMERGING FROM COLLISIONS OF COLD MAGNETIC ATOMS

Random Matrix Theory developed by Wigner to describe the statistics of eigenvalues (and eigenfunctions) of quantum many body systems (Wigner, 1955) for heavy nuclei with a large number of degrees of freedom has seen application in various physical problems ranging from fluctuations in spectra of atomic nuclei or molecules (Guhr et al., 1998), through statistical fluctuations observed in scattering processes for these systems, to quantum optics and condensed matter physics (Beenakker, 2001).

Quantum systems manifesting chaotic properties can be classified based on the nearest-neighbor spacing distribution (NNSD) of their eigenvalues (or observed resonances). The distribution of the spacings can be used to characterize the spectral fluctuations and is closely connected with absence or presence of correlation between energy levels. In case of non-interacting energy levels, the NNSD is Poissonian:

$$P_P(s) = \exp(-s),$$

where s is the normalized nearest neighbor spacing. If the interaction between energy levels is very strong, the NNSD is best described by fully chaotic Wigner-Dyson statistics (Wigner surmise) (Podolskiy and Narimanov, 2007):

$$P_{WD}(s) = \frac{\pi}{2} s \exp(-\frac{\pi}{4} s^2),$$

where the strong repulsion between energy levels is reflected in $P_{WD}(0) = 0$. The intermediate, partially chaotic cases (Karremans et al., 1998; Sakhr and Nieminen, 2005), are best described by Brody distribution (Brody, 1973):

$$P_B(\nu, s) = (1+\nu)\alpha s^{\nu} \exp(-\alpha s^{\nu+1}), \tag{18}$$

where $\alpha = [\Gamma((\nu+2)/(\nu+1))]^{\nu+1}$ and ν is the Brody parameter that serves as a measure of the chaos in the spectrum. Random, non-chaotic, Poisson spectrum corresponds to $\nu = 0$, while a fully chaotic spectrum, whose levels have characteristics of the eigenvalues of matrices from the Gaussian orthogonal ensemble (GOE), corresponds to the $\nu = 1$.

Theoretical calculations and corresponding experiments show emergence of chaos in complex triatomic systems such as Ar_3 (Leitner et al., 1989) or in reactive scattering of atoms and dimers (Croft et al., 2017). For diatomic molecules, the presence of chaotic behavior is less

obvious due to lesser complexity of these systems. Ultracold dipolar gases, due to inherent anisotropic interactions, have proved to be suitable systems for tests of exotic phenomena in few-body (Bohn et al., 2009; Wang et al., 2011; Mayle et al., 2012; Croft and Bohn, 2014) or many body physics (Ni et al., 2010; Baranov et al., 2012; Kadau et al., 2016), quantum computation (DeMille, 2002; Yelin et al., 2006; Carr et al., 2009) and ultracold chemistry (Quéméner and Julienne, 2012; Miranda et al., 2011; Pérez-Ríos et al., 2014). Recently, manifestations of quantum chaos were reported in collisions of ultracold dysprosium and erbium atoms (Maier et al., 2015b; Frisch et al., 2014; Maier et al., 2015a; Aikawa et al., 2012; Baumann et al., 2014). The nearest-neighbor spacings statistics applied on measured dense spectrum of Fano-Freshbach resonances was very close to Wigner-Dyson distribution (Frisch et al., 2014). In this case, the chaotic behavior of the measured spectra arises from the states that lie energetically just below the dissociation threshold of the dysprosium (or erbium) dimers. These experiments prompted Yang et al., 2017 to investigate the correspondence between classical and quantum chaos in ultracold collisions of dipolar molecules.

As my calculation were inspired by experiments on ultracold erbium and dysprosium atoms, I will briefly describe them. In a standard procedure found e.g. in Aikawa et al. (2012) and Frisch et al. (2014), the atoms are precooled in the magneto-optical trap and then loaded in an optical dipole trap, where the atoms are further cooled by evaporative cooling just slightly above the temperature needed for Bose-Einstein condensation. The trap then contains $\sim 10^5$ atoms with typical number densities of $\sim 10^{13}$ cm^{-3} and temperature on the order of hundreds of nanoKelvin. The probing magnetic field is then ramped up to a desired value and after set time suddenly switched off. The number of atoms and the cloud size is then measured by absorption imaging. The typical atom loss spectra of Fano-Feshbach

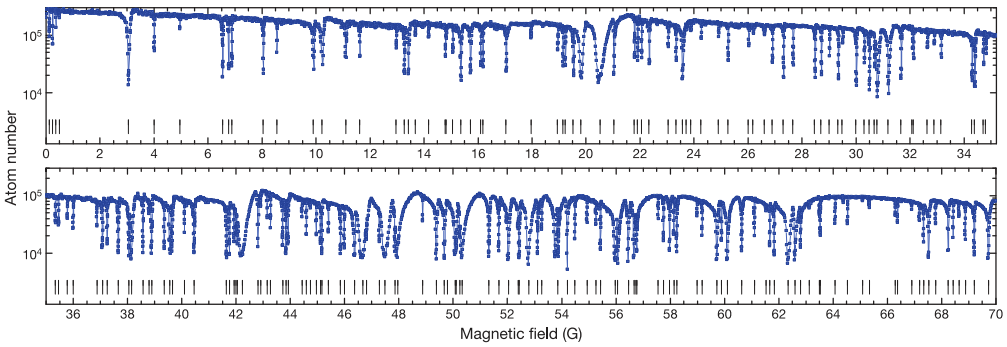

Figure 14: Fano-Feshbach spectrum of ^{166}Er in the energetically lowest Zeeman sublevel from 0 to 70 G as measured at temperature of 330 nK by Frisch et al. (2014) using trap-loss spectroscopy. The figure was adapted from the mentioned publication. Resonance positions are denoted by vertical lines.

resonances as measured by Frisch et al. (2014) are plotted in Fig. 14. At certain values of probing magnetic field some of the states of the dimer (see Fig. 15) are so close to the dissociation threshold so that the weakly bound dimer can be formed in collision of ultracold erbium (or dysprosium) atoms. This is accompanied by measured loss of the atoms in the trap.

We first used a simplified model for erbium and dysprosium dimers taking into account the features of about the right scale and quality. In our approximation the basic structure of rovibrational energy levels and spins is separated from the strong anisotropic couplings that are responsible for the emergence of chaos in the studied systems.

The model Hamilton operator describing a pair of ^{162}Dy atoms (in an external magnetic field) is taken to be

$$H = -\frac{\hbar^2}{2m_r}\left(\frac{d^2}{dR^2} - \frac{\mathbf{L}^2}{R^2}\right) + H_1 + H_2 + V_{int} \equiv H_{diag} + V_{int}\,, \qquad (19)$$

where m_r is the reduced mass of the atom pair, $\mathbf{R} = R\hat{R}$ describes the orientation of and the distance between the two atoms in relative coordinates, $\mathbf{L}^2$ is the squared partial wave angular momentum operator, V_{int} is regarded as interaction Hamiltonian that hold the molecule together and that engenders chaos in the spectra, and H_1 and H_2 are

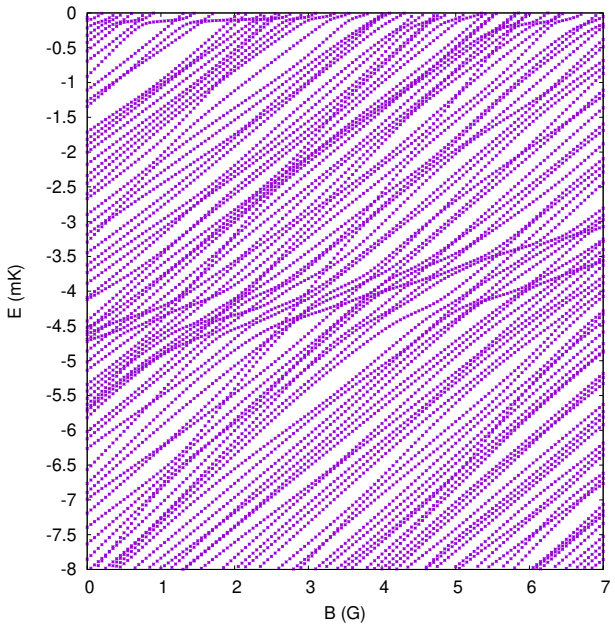

Figure 15: Adapted from Ref. Augustovičová and Bohn (2018a): Simulated spectrum of Dy_2 molecules, versus magnetic field, generated as described in the text. Each energy level at $B = 0$ evolves as the magnetic field is increased, eventually finding its way to zero energy, where it appears as a scattering resonance.

the internal Hamiltonians of the individual atoms, which depend in general on a magnetic field.

Specifically, the interaction term V_{int} is taken to include an isotropic contribution $V_{iso}(R)$ as well as anisotropic contributions, $V_{dd}(\mathbf{R})$ and $V_{ad}(\mathbf{R})$, that also depend on the orientation of the interatomic axis. The isotropic interaction describes an approximately correct long-range van der Waals interaction of Dy_2 with dispersion coefficient $C_6 = 2003$ au (Maier et al., 2015a). This potential is closed off at short range and it has an attractive well with depth 785.7 cm^{-1} (Petrov et al., 2012) to allow the calculation of rovibrational levels. The two total angular momenta $\mathbf{j}_1$, $\mathbf{j}_2$ of magnetic atoms interact via a long-range magnetic dipole-dipole interaction of the form

$$V_{dd}(\mathbf{R}) = \left(\frac{g\alpha}{2}\right)^2 \frac{\mathbf{j}_1 \cdot \mathbf{j}_2 - 3\,(\hat{R}\cdot\mathbf{j}_1)(\hat{R}\cdot\mathbf{j}_2)}{R^3}\,, \tag{20}$$

where α is the fine structure constant, g is the g-factor for the ground $^5I_8$ state of the Dy atom, whose value is $g = 1.2508$ (Judd and Lindgren, 1961), and $j_1 = j_2 = 8$. Furthermore, an anisotropic van der Waals interaction is an expansion in the dipole-dipole interaction given to first order by (Petrov et al., 2012)

$$V_{ad}(\mathbf{R}) = \frac{C_{ad}}{\sqrt{6}} \sum_{i=1}^{2} \frac{\mathbf{j}_i \cdot \mathbf{j}_i - 3\,(\hat{R}\cdot\mathbf{j}_i)(\hat{R}\cdot\mathbf{j}_i)}{R^6}\,, \tag{21}$$

where the coefficient C_{ad} sets the strength of this anisotropic dispersion interaction. It has been observed previously that V_{dd} is primarily responsible for anisotropic coupling in Dy_2, while V_{ad} is more important for Er_2 (Maier et al., 2015b; Yang et al., 2017).

The Hamiltonian matrix can be constructed and diagonalized for any desired value of magnetic field B. Fig. 15 shows the resulting map of molecular binding energies versus B. The intersections of the bound-state spectrum with the $E = 0$ axis indicate crossings of molecular levels with the threshold of two atoms in their lowest Zeeman sublevels $m_j = -8$ and correspond to the Fano-Feshbach resonance locations.

Given the resolution of the experiments (Frisch et al., 2014; Maier et al., 2015a) some of the very narrow Fano-Feshbach resonances could have been unobserved. In our theoretical calculations we are able to resolve all resonances and the Brody parameter is used solely as a measure of chaos. The histogram taken for calculated energy spectrum at zero magnetic field was best fitted with Brody parameter $\nu_E = 1^{+0}_{-0.23}$, while for the histogram drawn for magnetic field spectrum (i.e. Fano-Feshbach resonace spectrum) at $E = 0$ (dissociation threshold energy) we obtained Brody parameter $\nu_B = 0.93^{+0.07}_{-0.28}$ (see Figures 2a and 2b in Augustovičová and Bohn (2018a) for details). Both histograms of the NNS distributions were generated from 250 levels of the spectrum. The stated uncertainties are 1-σ uncertainties

arising from the fit of the data to the Brody functions (18), and are mainly given by the counting statistics of data in the histogram. Both spectra are chaotic to a high degree and the chaotic behavior is preserved in the mapping from energy to magnetic field spectra. It is necessary to note, that large statistical uncertainties of our calculations limit the quantitative precision of our results. Nevertheless, within these uncertainties, the obtained value of ν_B is almost consistent, albeit somewhat higher than the values of ~ 0.5–0.75 reported for the original ^{164}Dy data (Maier et al., 2015b).

Here it is important to note that the degree of chaos in the experimental data could have been underestimated due to difficulty to detect very narrow resonances. Mur-Petit and Molina (2015) made a new analysis of the original erbium data (Frisch et al., 2014) and concluded that the nearest neighbor spacing distribution is probably underestimating the chaoticity of the system if some of the levels were too narrow to be observed in the spectra. They found out that the data of Frisch et al. (2014) were consistent with a fraction of missing levels of $20-25\,\%$ with minimum widths of the missing resonances of about 10 mG. Their result hinted that the spectrum was in indeed chaotic but the original analysis was marred by insufficient resolution.

A single statistical evaluation as described above results in relatively large error bars. In order to get more accurate estimates of the corresponding Brody parameters we employ the random matrix theory of Wigner (1955). In this approach, the nonzero matrix elements of V_{int} of a chaotic molecule are represented by random variables with normal distribution cantered around zero with a variance of w_0. In such simulation, a more general description of the molecule can be achieved using the matrix elements with a distribution given by the probability density function (Życzkowski et al., 1992)

$$\begin{aligned} P(w, V_{ii}) &= \frac{1}{\sqrt{2\pi}\, w} \exp\left(-\frac{V_{ii}^2}{2w^2}\right), \\ P(w, V_{ij}) &= \frac{1}{\sqrt{\pi}\, w} \exp\left(-\frac{V_{ij}^2}{w^2}\right), \quad i \neq j. \end{aligned} \tag{22}$$

The variance w_0 in this approximate model of Dy_2 molecule is determined from the root-mean-squared variances calculated from the exact non-zero matrix elements. For the $^{164}Dy_2$ molecule, the calculated width $w_0 = 24.7$ mK. To construct the interaction matrix, the elements that are not zero due to symmetry are filled with random variables described by the GOE distribution (22). The elements of diagonal matrix H_{diag} in Eq. (19) are treated in the same way as in the exact calculation. We then performed a statistical analysis of many generated realizations of models of Dy_2 molecule to obtain an ensemble of independent Brody parameters. This set is further averaged to reduce the uncertainty, while approximately 30 realizations are necessary to decrease the determined uncertainty below $5\,\%$. The obtained

Brody parameters were $\nu_E = 0.94 \pm 0.05$, and $\nu_B = 0.98 \pm 0.05$, respectively. This indicates that the approximate model of the Dy_2 molecule is fully chaotic both in energy and magnetic field (i.e. Fano-Feshbach resonance) spectra.

My numerical and semianalytic results have shown that molecule exhibiting partial chaos in its energy spectrum below dissociation threshold can exhibit a similar or even greater degree of chaos in its spectrum of Fano-Feshbach resonances. To sum it up, in the discussed models, the transition from the energies at zero magnetic field to the Fano-Feshbach resonance spectrum at threshold energy involves either a number of avoided crossings or magnetic moment fluctuations of the molecular states that are not trivial in their nature.

5

CONCLUDING REMARKS

From the above overview of the studied problems and the accompanying publications it follows that the author has achieved the original results in the following areas:

I have investigated the radiative depopulation of helium metastable states 2^3S and 2^1S in collisions with helium, hydrogen and lithium ions within a fully quantum framework. Contrary to general expectation that these processes are governed by dipole moment interactions, I have discovered that in case of He_2^+ formation the radiative association driven by quadrupole moment is as important as that driven by dipole moment. This is the first time such observation was done for this kind of interactions. The comprehensive results on radiative processes involving primordial species can help to improve understanding of chemical evolution of the early Universe and shed more insight on the formation of the first molecules.

Several promising molecular systems were investigated in the search for a possible cosmological variation of proton to electron mass ratio. Actual calculations performed for diatomic hydride radicals revealed that particular energy levels pairs of diatomic radicals can be tuned to degeneracy by means of strong magnetic fields that prevail in many stellar and protostellar objects and that are achievable in the laboratory as well. I have shown that Zeeman tuning allows for a dramatic enhancement of the mass sensitivity coefficients of the involved transitions and also for a substantial reduction of their spectral line broadenings. Moreover, the tuned transitions exhibit favorable intensities, and therefore are being eminently suitable for radioastronomy observations. These findings could possibly result in more stringent constraints on m_p/m_e variation. Currently, I am trying to extend the approach to handle a broader range of classes of molecular transitions.

I have found and explained an effect that a combination of electric and magnetic field greatly enhances the prospect of evaporative cooling for polar molecules colliding in an appropriate state. In case of CaOH molecule I have shown that utilization of this technique can lead to temperatures in nanoKelvin range. A group of scientists led by prof. Doyle at Harvard University is currently attempting to use this proposed procedure to prepare an ultracold sample of CaOH

molecules, which may in the future lead to the development of an extremely precise molecular spectroscopy technique or to the formation of a previously unseen molecular Bose-Einstein condensate. There are several molecules, such as $CaOCH_3$ that seem to be promising with respect to possibility of their evaporative cooling and the respective calculations are in progress.

I have shown that for ultracold magnetic lanthanide atoms the chaotic scattering emerges due to a combination of anisotropic interaction potentials and Zeeman coupling under an external magnetic field. Several unique features of colliding magnetic lanthanides that have not been observed in any other ultracold atomic system were also discussed. An interesting observation was that molecule exhibiting partial chaos in its energy spectrum below dissociation threshold can exhibit a similar or even greater degree of chaos in its spectrum of Fano-Feshbach resonances.

Finally, I would like to point out that the covered topics are far from exhausted and many outstanding questions remain. The ongoing research is pursued not only by me, my coworkers and students but also by several theoretical and experimental groups abroad. The nature of the studied phenomena is such that international cooperation is crucial for further progress in the field.

A

MOLECULAR DESCRIPTION AND THEORY DETAILS: OH

A.1 MOLECULAR HAMILTONIAN IN THE ABSENCE OF FIELD

The zero-field Hamiltonian for the OH molecule in the $X\,^2\Pi$ electronic ground state can be written as (Brown et al., 1978)

$$H = H_0 + H_{rot} + H_{fs} + H_{hfs} \tag{23}$$

where H_0 denotes the nonrelativistic Hamiltonian of the nonrotating molecule, the nuclear rotational energy operator H_{rot} represents the angular momentum of the rigid nuclear framework, the term H_{fs} describes the fine structure interactions, and H_{hfs} contains terms associated with nuclear spin and nuclear moments known as hyperfine interactions. In the Born-Oppenheimer approximation the first term represents energy of vibrational levels E_{v_i} with vibrational wave functions $v_i(r)$. The explicit form of the other terms in a Hund's case (a) representation are the following:

$$H_{rot} = B(r)\mathbf{N}^2,$$

where $\mathbf{N} = \mathbf{J} - \mathbf{S}$ and $B(r) = \hbar^2/(2\mu r)$, μ is the reduced mass of the nuclei.

$$\begin{aligned} H_{fs} = {} & A(r)T^1_{q=0}(\mathbf{L})T^1_{q=0}(\mathbf{S}) + \gamma(r)(\mathbf{J}-\mathbf{S})\cdot\mathbf{S} \\ & + \sum_{q=\pm1} \exp(-2iq\phi)\left[-q_\Lambda(r)T^2_{2q}(\mathbf{J},\mathbf{J}) + (p_\Lambda(r) + 2q_\Lambda(r))\,T^2_{2q}(\mathbf{J},\mathbf{S})\right], \end{aligned}$$

where $A(r)$ is the spin-orbit coupling function, $\gamma(r)$ is the spin-rotation coupling parameter, and $p(r), q_\Lambda(r)$ are Λ-doubling parameters, ϕ is the electron orbital azimuthal angle.

$$\begin{aligned} H_{hfs} = {} & a(r)T^1_{q=0}(\mathbf{I})T^1_{q=0}(\mathbf{L}) + b_F(r)\mathbf{I}\cdot\mathbf{S} + \sqrt{\frac{2}{3}}c(r)T^2_{q=0}(\mathbf{I},\mathbf{S}) \\ & + d(r)\sum_{q=\pm1}\exp(-2iq\phi)T^2_{2q}(\mathbf{I},\mathbf{S}), \end{aligned}$$

Similarly as in the DUO approach (Yurchenko et al., 2016; Semenov et al., 2016), we treat the full Hamiltonian (23) variationally, so that the eigenstates of H_0 are vibronic states $|v(r), |\Lambda|, S\rangle$ and the effective Hamiltonian $H_{eff} = H - H_0$ is evaluated in this basis set getting

$$X_{v,v'} = \langle v_i(r)|X(r)|v'_j(r)\rangle \;\text{ for }\; X = A, B, \gamma, p_\Lambda, q_\Lambda, a, b_F, c, d, \tag{24}$$

where $i, j = 0, 1, \ldots$

The vibrational basis set functions v_i were obtained by solving the Schrödinger equation for H_0 using the effective potential energy curve which was obtained by morphing the ab initio potential energy curve of (Loo and Groenenboom, 2007) within the framework of the reduced potential energy curve approach (see e.g., Špirko, 2016) by fitting the experimental vibrational energies (Abrams et al., 1994). The resulting vibrational energies are shown in Table S1 in the Supplementary Material of Ref. Augustovičová and Špirko, 2020.

The radial independent tensorial terms of Hamiltonian H_{eff} are set up in hyperfine-rotational uncoupled $|J, M_J, L, S, \Omega, \Sigma, \Lambda\rangle|IM_I\rangle$ Hund's case (a) basis set, where $L = 1, S = 1/2$; Λ, Σ are a projection of **L**, **S** onto the molecule's axis, respectively. The spin-orbit interaction splits the $^2\Pi$ electronic state into two components, which are characterized by the quantum number $|\Omega|$, where $\Omega = \Lambda + \Sigma$, while $|\Omega| = 3/2$ is the energetically lower component and $|\Omega| = 1/2$ is the upper one. The total angular momentum without nuclear spin $J \geqslant |\Omega|$, and $I = 1/2$ for ^{16}OH. These states are combined into symmetrized eigenstates constructed from linear combinations of $|\pm|\Omega|\rangle$

$$\begin{aligned} &||\Lambda|, J, M_J, |\Omega|, I, M_I, \epsilon\rangle \qquad (25)\\ &\quad = \frac{1}{\sqrt{2}}\Big(||\Lambda|, J, M_J, |\Omega|, I, M_I\rangle + \epsilon(-1)^{J-S}|-|\Lambda|, J, M_J, -|\Omega|, I, M_I\rangle\Big) \end{aligned}$$

with the total parity under the inversion operation E^* for each rotational level. These functions can also be classified according to rotationless $p = e/f$-symmetry, total parity exclusive of a $(-1)^{J-1/2}$ factor, i.e. total wave functions with well-defined p-parity can therefore be

$$\begin{aligned} &|v(r), |\Lambda|; J, M_J, |\Omega|, I, M_I, {}^{e}_{f}\rangle\\ &\quad = \frac{1}{\sqrt{2}}\Big(|v(r), |\Lambda|; J, M_J, |\Omega|, I, M_I\rangle \pm |v(r), -|\Lambda|; J, M_J, -|\Omega|, I, M_I\rangle\Big). \end{aligned}$$

The spectroscopic constants $X_{v,v'}$ in (24) entering the effective Hamiltonian H_{eff} (see Table S2 and S3 in the Supplementary Material of Ref. Augustovičová and Špirko, 2020) were obtained by morphing their $X(r)$ approximants expressed as rational functions and by a direct nonlinear fitting the measured line frequencies for Λ-type doubling hyperfine transitions (Amano, 1984; Meerts and Dymanus, 1975; Dousmanis et al., 1955; Radford, 1968; Ball et al., 1970; Coxon et al., 1979; Ter Meulen and Dymanus, 1972; Ter Meulen et al., 1976; Destombes and Marlière, 1975; Destombes et al., 1979; Kolbe et al., 1981) and hyperfine-resolved rotational transitions (Varberg and Evenson, 1993; Blake et al., 1986; Farhoomand et al., 1985). With an exception for $\gamma(r)$, the functional forms of the morphed approximants were deduced from the available ab initio data (Loo and Groenenboom, 2007; Langhoff and Partridge, 1984; Kristiansen and Veseth, 1986): $\gamma(r)$ was assumed to be a linear function in r. To allow for evaluation of the mass dependence of the molecular states, the mass

dependence of each of the Hamiltonian terms was respected explicitly.

A.2 ZEEMAN HAMILTONIAN

If a homogenous magnetic field is applied the molecular magnetic moment interacts with the field and as a result the energy levels are shifted due to the Zeeman effect, with the Zeeman interaction Hamiltonian operator $H_Z = -\boldsymbol{\mu}_s \cdot \mathbf{B}$, where $\boldsymbol{\mu}_s$ is the magnetic moment in the space-fixed reference frame. The magnetic moment of the $|\Omega| = 3/2$ state is large in contrast with the $|\Omega| = 1/2$ state for which the orbital and spin contribution to the molecular magnetic moment nearly cancel. Magnetic field $\mathbf{B}$ is chosen along the space-fixed Z-axis.

The field-free Hamiltonian H is invariant under any rotation of the space fixed axis system, hence the total angular momentum including nuclear spin and its component relative to the space-fixed Z axis, F, M_F (in the coupling scheme $\mathbf{F} = \mathbf{J} + \mathbf{I}$, where the nuclear spin of the hydrogen nucleus $\mathbf{J}$ is coupled with the rotational angular momentum $\mathbf{J}$) are good quantum numbers. The total parity ϵ as a good quantum label was mentioned earlier. The symmetries of the system are further reduced when an external magnetic field is applied. The term H_Z is not, however, totally symmetric in the group of spatial three-dimensional pure rotations but it is invariant under arbitrary rotation about the direction of $\mathbf{B}$. In other words the symmetries of H_Z includes precession about the Z axis and inversion of the spatial coordinates of all atoms in a molecule, thus M_F and ϵ remain good quantum numbers.

We adopted the Zeeman Hamiltonian for a diatomic molecule, which contains the isotropic electron spin Zeeman effect, the electron orbital Zeeman effect, the rotational Zeeman effect, the anisotropic electron spin Zeeman effect, the nuclear spin Zeeman effect, extended to the Λ-doubling Zeeman terms for Π molecules (Brown et al., 1978)

$$\begin{aligned} H_Z = \mu_0 B \Big[& g_S T^1_{p=0}(\mathbf{S}) + g_L T^1_{p=0}(\mathbf{L}) - g_r(r) T^1_{p=0}(\mathbf{J}-\mathbf{L}-\mathbf{S}) \\ & + g_l \sum_{q=\pm 1} D^1_{0q}(\omega)^* T^1_q(\mathbf{S}) \\ & - g'_l \sum_{q=\pm 1} e^{-2iq\phi} D^1_{0-q}(\omega)^* T^1_q(\mathbf{S}) \\ & - g^{e'}_r \sum_{q=\pm 1} \sum_p e^{-2iq\phi} (-1)^p D^1_{-p-q}(\omega)^* T^1_q(\mathbf{J}-\mathbf{S}) \Big] \\ & - \mu_N B g_N T^1_{p=0}(\mathbf{I}) - \frac{1}{2} T^2\big(\chi(r)\big) T^2(\mathbf{B},\mathbf{B}), \end{aligned}$$

where μ_0 is the Bohr magneton, μ_N is the nuclear magneton, g_S is the electron spin g-factor, g_L is the electron orbital g-factor, g_r is the rotational g-factor, g_N is the nuclear spin g-factor, and χ is the magnetic susceptibility (Ramos and Bueno, 2006; Flygare, 1974). Note that

a reliable determination of the functions $g_r(r)$ and $\chi(r)$ for open-shell molecules appears as still infeasible. However, for fields weaker than $\sim 10^6$ Gauss, $g_r(r)$ can be treated as a constant and $\chi(r)$ safely neglected (Angel and Landstreet, 1974); in this study we rely on $g_S = 2.00152$, $g_L = 1.00107$ $g_r = -0.000633$, $g_l = 0.00400, g_l' = 0.006386$, $g_r^{e'} = 0.0020446$ (Brown et al., 1978), and χ=0.

The sought energies of ^{16}OH in a homogenous magnetic field **B** were obtained by diagonalizing the total Hamiltonian $H + H_Z$ as a matrix in the basis (25).

A.3 ESTIMATIONS OF TRANSITION INTENSITIES

The probability of an electric and magnetic dipole transitions from an initial state $|\psi\rangle$ to a final state $|\psi'\rangle$ is proportional to the square of the transition matrix element $\langle\psi|T^1_p(\mu_s^{el/mag})|\psi'\rangle$ times a cube of the transition frequency. The spherical irreducible tensor operator of the dipole moment transforms under rotation of the coordinate frame as

$$T^1_p(\mu_s^{el/mag}) = \sum_q D^1_{pq}(\omega)^* T^1_q(\mu_m^{el/mag}),$$

where $D^1_{pq}(\omega)$ are elements of Wigner rotation matrix, ω is a general symbol for a set of three Euler angles. Using a direct product wave function $|(JI)\,\Omega, F, M_F\rangle|\nu;\Lambda, S, \Sigma\rangle|$, we can separate the rotational part involved only by the Wigner D-matrix and vibronic part involved only by $T^1_q(\mu_m^{el/mag})$. Employing the Wigner-Eckart theorem we can calculate the rotational matrix element as Brink and Satchler (1994)

$$\begin{aligned}&\langle(JI)\,\Omega, F, M_F|D^1_{pq}(\omega)^*|(J'I)\,\Omega', F', M_F'\rangle \\ &\quad = (-1)^{F+F'+\Omega+I-M_F+1}[F][F'][J][J'] \\ &\qquad \times \begin{pmatrix} F & 1 & F' \\ -M_F & p & M_F' \end{pmatrix} \begin{Bmatrix} F & F' & 1 \\ J' & J & I \end{Bmatrix} \begin{pmatrix} J & 1 & J' \\ -\Omega & q & \Omega' \end{pmatrix},\end{aligned}$$

where $[F] = \sqrt{2F+1}$ etc. The vibrational transition moment $\langle\nu;\Lambda, S, \Sigma|T^1_q(\mu_m^{el/mag})|\nu;\Lambda', S, \Sigma'\rangle\delta_{\Sigma'\Sigma}\delta_{\Lambda'\Lambda}$ for the ground electronic state varies with vibrational quantum number only weakly (Loo and Groenenboom, 2007), therefore we can assume a constant value taken as one for the purpose of the relative intensities determination:

$$I_{rel}^{el/mag} \propto |\langle J, M_J, |\Omega|, I, M_I, p|D^1_{pq}(\omega)^*|J', M_J', |\Omega'|, I, M_I', p'\rangle|^2,$$

where the transformation from coupled to uncoupled representation is given as usual via Clebsch-Gordan coefficients

$$|J, M_J, \Omega, I, M_I\rangle = \sum_{F=|J-I|}^{J+I} \sum_{M_F=-F}^{F} |(JI)\,\Omega, F, M_F\rangle\langle F, M_F|JM_JIM_I\rangle.$$

BIBLIOGRAPHY

Abrams, M. C., S. P. Davis, M. L. P. Rao, R. Engleman Jr., and J. W. Brault (1994). "High-resolution Fourier transform spectroscopy of the Meinel system of OH." In: *Astrophys. J. Suppl. Ser.* 93, pp. 351–395 (cit. on p. 54).
DOI: 10.1086/192058.

Aikawa, K., A. Frisch, M. Mark, S. Baier, A. Rietzler, R. Grimm, and F. Ferlaino (2012). "Bose-Einstein Condensation of Erbium." In: *Phys. Rev. Lett.* 108 (21), p. 210401 (cit. on p. 46).
DOI: 10.1103/PhysRevLett.108.210401.

Amano, T. (1984). "Difference frequency laser spectroscopy of OH and OD: Simultaneous fit of the infrared and microwave lines." In: *J. Mol. Spectrosc.* 103.2, pp. 436–454 (cit. on p. 54).
DOI: https://doi.org/10.1016/0022-2852(84)90067-5.

Anderegg, L., B. L. Augenbraun, Y. Bao, S. Burchesky, L. W. Cheuk, W. Ketterle, and J. M. Doyle (2018). "Laser cooling of optically trapped molecules." In: *Nature Physics* 14.9, pp. 890–893 (cit. on p. 36).
DOI: 10.1038/s41567-018-0191-z.

Angel, J. R. P. and J. D. Landstreet (1974). "A Determination by the Zeeman Effect of the Magnetic Field Strength in the White Dwarf G99-37." In: *Astrophys. J.* 191, pp. 457–464 (cit. on p. 56).
DOI: 10.1086/152984.

Augenbraun, B. L., Z. D. Lasner, A. Frenett, H. Sawaoka, C. Miller, T. C. Steimle, and J. M. Doyle (2020). "Laser-cooled polyatomic molecules for improved electron electric dipole moment searches." In: *New Journal of Physics* 22.2, p. 022003 (cit. on p. 38).
DOI: 10.1088/1367-2630/ab687b.

Augustovičová, L. (2011). "Radiative association of atoms." MA thesis. Czech Technical University in Prague, Faculty of Nuclear Sciences and Physical Engineering (cit. on p. 15).

Augustovičová, L. (2014). *Quantum dynamics of small molecules*. Dissertation thesis. Faculty of Mathematics and Physics, Charles University (cit. on p. 14).

Augustovičová, L., W. P. Kraemer, and P. Soldán (2014a). "Depopulation of metastable helium by radiative association with hydrogen and lithium ions." In: *Astrophys. J.* 782, p. 46 (cit. on pp. 14, 17, 18, 20, 24, 25).
DOI: 10.1088/0004-637X/782/1/46.

Augustovičová, L., W. P. Kraemer, and P. Soldán (2014b). "Depopulation of metastable helium He(2^1S) by radiative association with

hydrogen and lithium cations." In: *J. Quant. Spec. Rad. Trans.*, 148. accepted, pp. 27–37 (cit. on pp. 14, 17–19, 24, 25).
DOI: 10.1016/j.jqsrt.2014.06.012.

Augustovičová, L., W. P. Kraemer, V. Špirko, and P. Soldán (2015a). "The role of molecular quadrupole transitions in the depopulation of metastable helium." In: *Mon. Not. R. Astron. Soc.* 446, pp. 2738–2743 (cit. on pp. 14, 18, 21–24).
DOI: 10.1093/mnras/stu2317.

Augustovičová, L., P. Soldán, W. P. Kraemer, and V. Špirko (2014c). "Potential microwave probes of the proton-to-electron mass ratio at very high redshifts." In: *Mon. Not. R. Astron. Soc.* 439, pp. 1136–1139 (cit. on pp. 12, 29–31).
DOI: 10.1093/mnras/stu060.

Augustovičová, L., P. Soldán, and V. Špirko (2016). "Effective hyperfine structure functions of ammonia." In: *The Astrophysical Journal* 824, p. 147 (cit. on pp. 28, 31).
DOI: 10.3847/0004-637x/824/2/147.

Augustovičová, L., V. Špirko, W. P. Kraemer, and P. Soldán (2012). "Radiative association of $LiHe^+$." In: *Chem. Phys. Lett.* 531, pp. 59–63 (cit. on pp. 14, 16, 20, 24, 25).
DOI: 10.1016/j.cplett.2012.02.038.

Augustovičová, L., V. Špirko, W. P. Kraemer, and P. Soldán (2013a). "Radiative association of He_2^+ revisited." In: *Astron. Astrophys.* 553, A42 (cit. on pp. 14, 16).
DOI: 10.1088/0004-637X/749/1/22.

Augustovičová, L., V. Špirko, W. P. Kraemer, and P. Soldán (2013b). "Radiative association of He_2^+: the role of quartet states." In: *Mon. Not. R. Astron. Soc.* 435, pp. 1541–1546 (cit. on pp. 14, 17).
DOI: 10.1093/mnras/stt1395.

Augustovičová, L. D. and J. L. Bohn (2017). "No evaporative cooling of nitric oxide in its ground state." In: *Phys. Rev. A* 96, p. 042712 (cit. on pp. 40, 41).
DOI: 10.1103/PhysRevA.96.042712.

Augustovičová, L. D. and J. L. Bohn (2018a). "Manifestation of quantum chaos in Fano-Feshbach resonances." In: *Physical Review A* 98, p. 023419 (cit. on pp. 47, 48).
DOI: 10.1103/PhysRevA.98.023419.

Augustovičová, L. D. and J. L. Bohn (2018b). "NO evaporative cooling in the $^2\Pi_{3/2}$ state." In: *Phys. Rev. A* 97, p. 062703 (cit. on pp. 40, 41).
DOI: 10.1103/PhysRevA.97.062703.

Augustovičová, L. D. and J. L. Bohn (2019). "Ultracold collisions of polyatomic molecules: CaOH." In: *New Journal of Physics* 21.10, p. 103022 (cit. on pp. 38, 39, 42–44).
DOI: 10.1088/1367-2630/ab4720.

Augustovičová, L. D. and V. Špirko (2020). "Zeeman molecular probe for tests of fundamental physical constants." In: *Monthly Notices of the Royal Astronomical Society* 494.2, pp. 1675–1680 (cit. on pp. 33, 34, 54).
DOI: 10.1093/mnras/staa792.

Augustovičová, L., M. Zámečníková, W. P. Kraemer, and P. Soldán (2015b). "Radiative association of He(2^3P) with lithium cations." In: *Chemical Physics* 462. Inelastic Processes in Atomic, Molecular and Chemical Physics, pp. 65–70 (cit. on pp. 14, 17, 18).
DOI: 10.1016/j.chemphys.2015.07.003.

Avdeenkov, A. V. and J. L. Bohn (2002). "Collisional dynamics of ultracold OH molecules in an electrostatic field." In: *Phys. Rev. A* 66 (5), p. 052718 (cit. on p. 42).
DOI: 10.1103/PhysRevA.66.052718.

Babb, J. F. and A. Dalgarno (1995). "Radiative association and inverse predissociation of oxygen atoms." In: *Phys. Rev. A* 51, pp. 3021–3026 (cit. on p. 13).
DOI: 10.1103/PhysRevA.51.3021.

Bacchus-Montabonel, M.-C. and D. Talbi (1999). "A theoretical treatment of the LiH and BeH formation through radiative association." In: *J. Mol. Struct. (Theochem)* 463, pp. 91–97 (cit. on p. 14).
DOI: 10.1016/S0166-1280(98)00397-2.

Bagdonaite, J., M. Daprà, P. Jansen, H. L. Bethlem, W. Ubachs, S. Muller, C. Henkel, and K. M. Menten (2013a). "Robust Constraint on a Drifting Proton-to-Electron Mass Ratio at z=0.89 from Methanol Observation at Three Radio Telescopes." In: *Phys. Rev. Lett.* 111, p. 231101 (cit. on p. 28).
DOI: 10.1103/PhysRevLett.111.231101.

Bagdonaite, J., P. Jansen, C. Henkel, H. L. Bethlem, K. M. Menten, and W. Ubachs (2013b). "A stringent limit on a drifting proton-to-electron mass ratio from alcohol in the early Universe." In: *Science* 339, pp. 46–48 (cit. on p. 28).
DOI: 10.1126/science.1224898.

Ball, J. A., D. F. Dickinson, C. A. Gottlieb, and H. E. Radford (1970). "The 3.8-cm Spectrum of OH: Laboratory Measurement and Low-Noise Search in W3 (OH)." In: *The Astronomical Journal* 75, p. 762 (cit. on p. 54).
DOI: 10.1086/111022.

Baranov, M. A., M. Dalmonte, G. Pupillo, and P. Zoller (2012). "Condensed Matter Theory of Dipolar Quantum Gases." In: 112.9, pp. 5012–5061 (cit. on p. 46).
DOI: 10.1021/cr2003568.

Barry, J. F., D. J. McCarron, E. B. Norrgard, M. H. Steinecker, D. DeMille, J. F. Barry, D. J. McCarron, E. B. Norrgard, et al. (2014).

"Magneto-optical trapping of a diatomic molecule." In: *Nature* 512, pp. 286–289 (cit. on p. 36).
DOI: 10.1038/nature13634.

Bates, D. R. (1951). "Rate of formation of molecules by radiative association." In: *Mon. Not. R. Astron. Soc.* 111, pp. 303–314 (cit. on p. 13).
DOI: 10.1093/mnras/111.3.303.

Bates, D. R. and L. Spitzer (1951). "The density of molecules in interstellar space." In: *Astrophys. J.* 113, pp. 414–463 (cit. on p. 13).
DOI: 10.1086/145415.

Baumann, K., N. Q. Burdick, M. Lu, and B. L. Lev (2014). "Observation of low-field Fano-Feshbach resonances in ultracold gases of dysprosium." In: *Phys. Rev. A* 89 (2), p. 020701 (cit. on p. 46).
DOI: 10.1103/PhysRevA.89.020701.

Beenakker, C. W. J. (2001). *The Oxford Handbook of Random Matrix Theory*. Ed. by P. D. F. G. Akemann J. Baik. Oxford: Oxford University Press, pp. 723–758 (cit. on p. 45).

Belov, S., Š. Urban, and G. Winnewisser (1998). "Hyperfine Structure of Rotation-Inversion Levels in the Excited v_2 State of Ammonia." In: *Journal of Molecular Spectroscopy* 189.1, pp. 1–7 (cit. on p. 31).
DOI: https://doi.org/10.1006/jmsp.1997.7516.

Beloy, K., A. Borschevsky, P. Schwerdtfeger, and V. V. Flambaum (2010). "Enhanced sensitivity to the time variation of the fine-structure constant and m_p/m_e in diatomic molecules: A closer examination of silicon monobromide." In: *Phys. Rev. A* 82 (2), p. 022106 (cit. on p. 27).
DOI: 10.1103/PhysRevA.82.022106.

Belyaev, A. K., L. Augustovičová, P. Soldán, and W. P. Kraemer (2014). "Non-radiative inelastic processes in lithium-helium ion-atom collisions." In: *Astron. Astrophys.* 565, A106 (cit. on pp. 19, 24, 25).
DOI: 10.1051/0004-6361/201423578.

Belyaev, A. K., D. S. Rodionov, L. Augustovičová, P. Soldán, and W. P. Kraemer (2015). "Full quantum study of non-radiative inelastic processes in lithium–helium ion–atom collisions." In: *Mon. Not. R. Astron. Soc.* 449, pp. 3323–3332 (cit. on pp. 17, 24, 25).
DOI: 10.1093/mnras/stv391.

Bennett, O. J., A. S. Dickinson, T. Leininger, and F. X. Gadéa (2003). "Radiative association in Li+H revisited: the role of quasi-bound states." In: *Mon. Not. R. Astron. Soc.* 341, pp. 361–368 (cit. on p. 14).
DOI: 10.1111/j.1365-2966.2008.12586.x.

Bernath, P. F. (2005). *Spectra of Atoms and Molecules*. 2nd. New York: Oxford University Press (cit. on pp. 16, 17).

Bertone, G. (2013). *Particle Dark Matter: Observations, Models and Searches*. Cambridge, UK: Cambridge University Press (cit. on p. 26).

Beyer, M. and F. Merkt (2018). "Half-Collision Approach to Cold Chemistry: Shape Resonances, Elastic Scattering, and Radiative Association in the $H^+ + H$ and $D^+ + D$ Collision Systems." In: *Phys. Rev. X* 8, p. 031085 (cit. on p. 13).
DOI: 10.1103/PhysRevX.8.031085.

Bichsel, B. J., M. A. Morrison, N. Shafer-Ray, and E. R. I. Abraham (2007). "Experimental and theoretical investigation of the Stark effect for manipulating cold molecules: Application to nitric oxide." In: *Phys. Rev. A* 75, p. 023410 (cit. on p. 40).
DOI: 10.1103/PhysRevA.75.023410.

Blake, G. A., J. Farhoomand, and H. M. Pickett (1986). "The far-infrared rotational spectrum of $X^2\Pi$ OH." In: *J. Mol. Spectrosc.* 115.1, pp. 226–228 (cit. on p. 54).
DOI: https://doi.org/10.1016/0022-2852(86)90289-4.

Bohn, J. L., M. Cavagnero, and C. Ticknor (2009). "Quasi-universal dipolar scattering in cold and ultracold gases." In: *New Journal of Physics* 11.5, p. 055039 (cit. on p. 46).
DOI: 10.1088/1367-2630/11/5/055039.

Bohn, J. L. and D. S. Jin (Feb. 2014). "Differential scattering and rethermalization in ultracold dipolar gases." In: *Phys. Rev. A* 89 (2), p. 022702 (cit. on p. 36).
DOI: 10.1103/PhysRevA.89.022702.

Bohn, J. L., A. M. Rey, and J. Ye (2017). "Cold molecules: Progress in quantum engineering of chemistry and quantum matter." In: *Science* 357.6355, pp. 1002–1010 (cit. on p. 36).
DOI: 10.1126/science.aam6299.

Bovino, S., M. Tacconi, and F. A. Gianturco (2011). "Photon-induced evolutionary rates of $LiHe^+$ ($^1\Sigma^+$) in early Universe from accurate quantum computations." In: *Astrophys. J.* 740, p. 101 (cit. on p. 14).
DOI: 10.1088/0004-637X/740/2/101.

Brink, D. M. and G. R. Satchler (1994). *Angular Momentum*. 3rd. Oxford: Clarendon Press (cit. on p. 56).

Brody, T. A. (1973). "A statistical measure for the repulsion of energy levels." In: *Lett. Nuovo Cimento* 7.12, pp. 482–484 (cit. on p. 45).
DOI: 10.1007/BF02727859.

Brown, J., M. Kaise, C. Kerr, and D. Milton (1978). "A determination of fundamental Zeeman parameters for the OH radical." In: *Mol. Phys.* 36.2, pp. 553–582 (cit. on pp. 53, 55, 56).
DOI: 10.1080/00268977800101761.

Cahn, S. B., J. Ammon, E. Kirilov, Y. V. Gurevich, D. Murphree, R. Paolino, D. A. Rahmlow, M. G. Kozlov, et al. (2014). "Zeeman-Tuned Rotational Level-Crossing Spectroscopy in a Diatomic Free Radical." In: *Phys. Rev. Lett.* 112 (16), p. 163002 (cit. on p. 33).
DOI: 10.1103/PhysRevLett.112.163002.

Carr, L. D., D. DeMille, R. V. Krems, and J. Ye (2009). "Cold and ultracold molecules: science, technology and applications." In: *New Journal of Physics* 11.5, p. 055049 (cit. on p. 46).
DOI: 10.1088/1367-2630/11/5/055049.

Carrington, A. (1996). "Microwave spectroscopy at the dissociation limit." In: *Science* 274, pp. 1327–1331 (cit. on p. 30).
DOI: 10.1126/science.274.5291.1327.

Carrington, A., A. M. Shaw, and S. M. Taylor (1995). "Ion-beam spectroscopy of long-range complexes." In: *J. Chem. Soc. Faraday Trans.* 91, pp. 3725–3740 (cit. on p. 30).
DOI: 10.1039/ft9959103725.

Chae, E., L. Anderegg, B. L. Augenbraun, A. Ravi, B. Hemmerling, N. R. Hutzler, A. L. Collopy, J. Ye, et al. (2017). "One-dimensional magneto-optical compression of a cold CaF molecular beam." In: *New Journal of Physics* 19, p. 033035 (cit. on p. 36).
DOI: 10.1088/1367-2630/aa6470.

Cheuk, L. W., L. Anderegg, B. L. Augenbraun, Y. Bao, S. Burchesky, W. Ketterle, and J. M. Doyle (Aug. 2018). "~-Enhanced Imaging of Molecules in an Optical Trap." In: *Phys. Rev. Lett.* 121 (8), p. 083201 (cit. on p. 36).
DOI: 10.1103/PhysRevLett.121.083201.

Chin, C., V. V. Flambaum, and M. G. Kozlov (2009). "Ultracold molecules: new probes on the variation of fundamental constants." In: *New Journal of Physics* 11.5, p. 055048 (cit. on p. 27).
DOI: 10.1088/1367-2630/11/5/055048.

Chin, C. and V. V. Flambaum (2006). "Enhanced Sensitivity to Fundamental Constants In Ultracold Atomic and Molecular Systems near Feshbach Resonances." In: *Phys. Rev. Lett.* 96 (23), p. 230801 (cit. on p. 27).
DOI: 10.1103/PhysRevLett.96.230801.

Cooley, J. W. (1961). "An improved eigenvalue corrector formula for solving the Schrödinger equation for central fields." In: *Math. Comput.* 15, pp. 363–374 (cit. on p. 15).
DOI: 10.1090/S0025-5718-1961-0129566-X.

Coxon, J. A., K. V. L. N. Sastry, J. A. Austin, and D. H. Levy (1979). "The microwave spectrum of the OH $X^2\Pi$ radical in the ground and vibrationally-excited ($v \leqslant 6$) levels." In: *Canadian Journal of Physics* 57.5, pp. 619–634 (cit. on p. 54).
DOI: 10.1139/p79-089.

Croft, J. F. E., C. Makrides, M. Li, A. Petrov, B. K. Kendrick, N. Balakrishnan, and S. Kotochigova (2017). "Universality and chaoticity in ultracold K plus KRb chemical reactions." In: *Nature Communications* 8, p. 15897 (cit. on p. 45).
DOI: 10.1038/ncomms15897.

Croft, J. F. E. and J. L. Bohn (2014). "Long-lived complexes and chaos in ultracold molecular collisions." In: *Phys. Rev. A* 89 (1), p. 012714 (cit. on p. 46).
DOI: 10.1103/PhysRevA.89.012714.

Crutcher, R. M. (1999). "Magnetic Fields in Molecular Clouds: Observations Confront Theory." In: *The Astrophysical Journal* 520.2, pp. 706–713 (cit. on p. 33).
DOI: 10.1086/307483.

Crutcher, R. M. (2012). "Magnetic Fields in Molecular Clouds." In: *Annual Review of Astronomy and Astrophysics* 50.1, pp. 29–63 (cit. on p. 33).
DOI: 10.1146/annurev-astro-081811-125514.

Dalgarno, A., K. Kirby, and P. C. Stancil (1996). "The radiative association of Li^+ and H, Li and H^+, and Li and H." In: *Astrophys. J.* 458, pp. 397–400 (cit. on p. 13).
DOI: 10.1086/176823.

DeMille, D. (2002). "Quantum Computation with Trapped Polar Molecules." In: *Phys. Rev. Lett.* 88 (6), p. 067901 (cit. on p. 46).
DOI: 10.1103/PhysRevLett.88.067901.

Destombes, J., B. Lemoine, and C. Marlière-Demuynck (1979). "Microwave spectrum of the hydroxyl radical in the $v = 1$ $^2\Pi_{3/2}$ state." In: *Chem. Phys. Lett.* 60.3, pp. 493–495 (cit. on p. 54).
DOI: https://doi.org/10.1016/0009-2614(79)80619-3.

Destombes, J. and C. Marlière (1975). "Measurement of hyperfine splitting in the OH radical by a radio-frequency microwave double resonance method." In: *Chem. Phys. Lett.* 34.3, pp. 532–536 (cit. on p. 54).
DOI: https://doi.org/10.1016/0009-2614(75)85556-4.

Dickinson, A. S. (2005). "Radiative association of H and D." In: *J. Phys. B* 38, pp. 4329–4334 (cit. on p. 14).
DOI: 10.1088/0953-4075/38/23/014.

Dine, M. and A. Kusenko (2003). "Origin of the matter-antimatter asymmetry." In: *Rev. Mod. Phys.* 76 (1), pp. 1–30 (cit. on p. 26).
DOI: 10.1103/RevModPhys.76.1.

Dousmanis, G. C., T. M. Sanders, and C. H. Townes (1955). "Microwave Spectra of the Free Radicals OH and OD." In: *Phys. Rev.* 100 (6), pp. 1735–1754 (cit. on p. 54).
DOI: 10.1103/PhysRev.100.1735.

Drake, G. W. F. (1971). "Theory of relativistic magnetic dipole transitions: lifetime of the metastable 2^3S state of the heliumlike ions." In: *Phys. Rev. A* 3, pp. 908–915 (cit. on p. 13).
DOI: 10.1103/PhysRevA.3.908.

Elioff, M. S., J. J. Valentini, and D. W. Chandler (2003). "Subkelvin Cooling NO Molecules via "Billiard-like" Collisions with Argon." In: 302, pp. 1940–1943 (cit. on p. 40).
DOI: 10.1126/science.1090679.

Farhoomand, J., H. M. Pickett, and G. A. Blake (1985). "Direct measurement of the fundamental rotational transitions of the OH radical by laser sideband spectroscopy." In: *Astrophys. J. Lett.* 291, pp. L19–L22 (cit. on p. 54).
DOI: 10.1086/184450.

Flambaum, V. V. (2006). "Enhanced Effect of Temporal Variation of the Fine Structure Constant and the Strong Interaction in ^{229}Th." In: *Phys. Rev. Lett.* 97 (9), p. 092502 (cit. on p. 27).
DOI: 10.1103/PhysRevLett.97.092502.

Flambaum, V. V. and M. G. Kozlov (2007). "Enhanced Sensitivity to the Time Variation of the Fine-Structure Constant and m_p/m_e in Diatomic Molecules." In: *Phys. Rev. Lett.* 99 (15), p. 150801 (cit. on pp. 27, 28).
DOI: 10.1103/PhysRevLett.99.150801.

Flygare, W. H. (1974). "Magnetic interactions in molecules and an analysis of molecular electronic charge distribution from magnetic parameters." In: *Chemical Reviews* 74, pp. 653–687 (cit. on p. 55).
DOI: 10.1021/cr60292a003.

Frisch, A., M. Mark, K. Aikawa, F. Ferlaino, J. L. Bohn, C. Makrides, A. Petrov, and S. Kotochigova (2014). "Quantum chaos in ultracold collisions of gas-phase erbium atoms." In: *Nature* 507 (7493), p. 475 (cit. on pp. 46–49).
DOI: 10.1038/nature13137.

Gacesa, M. and R. Côté (2014). "Photoassociation of ultracold molecules near a Feshbach resonance as a probe of the electron–proton mass ratio variation." In: *J. Mol. Spectrosc.* 300. Spectroscopic Tests of Fundamental Physics, pp. 124–130 (cit. on p. 27).
DOI: https://doi.org/10.1016/j.jms.2014.03.005.

Gerlich, D. and S. Horning (1992). "Experimental investigation of radiative association processes as related to interstellar chemistry." In: *Chem. Rev.* 92, pp. 1509–1539 (cit. on p. 13).
DOI: 10.1021/cr00015a003.

Gerlich, D., P. Jusko, S. Roucka, I. Zymak, R. Plasil, and J. Glosik (2012). "Ion Trap Studies of $H^- + H \rightarrow H_2 + e^-$ Between 10 and 135 K." In: *Astrophys. J.* 749.1, 22, p. 22 (cit. on p. 12).
DOI: 10.1088/0004-637X/749/1/22.

Gianturco, F. A. and P. G. Giorgi (1996). "Radiative association of LiH ($X\ ^1\Sigma^+$) from electronically excited lithium atoms." In: *Phys. Rev. A* 54, pp. 4073–4077 (cit. on p. 14).
DOI: 10.1103/PhysRevA.54.4073.

Gianturco, F. A. and P. G. Giorgi (1997). "Radiative association rates and structure of resonances for Li and Li^+ colliding with H and H^+." In: *Astrophys. J.* 479, pp. 560–567 (cit. on p. 14).
DOI: 10.1086/303902.

Godun, R. M., P. B. R. Nisbet-Jones, J. M. Jones, S. A. King, L. A. M. Johnson, H. S. Margolis, K. Szymaniec, S. N. Lea, et al. (2014). "Frequency Ratio of Two Optical Clock Transitions in $^{171}Yb^{+}$ and Constraints on the Time Variation of Fundamental Constants." In: *Phys. Rev. Lett.* 113, p. 210801 (cit. on pp. 26, 28).
DOI: 10.1103/PhysRevLett.113.210801.

Guhr, T., A. Müller–Groeling, and H. A. Weidenmüller (1998). "Random-matrix theories in quantum physics: common concepts." In: *Physics Reports* 299.4, pp. 189–425 (cit. on p. 45).
DOI: https://doi.org/10.1016/S0370-1573(97)00088-4.

Güsten, R., H. Wiesemeyer, D. Neufeld, K. M. Menten, U. U. Graf, K. Jacobs, B. Klein, O. Ricken, et al. (2019). "Astrophysical detection of the helium hydride ion HeH^{+}." In: *Nature* 568.7752, pp. 357–359 (cit. on p. 12).
DOI: 10.1038/s41586-019-1090-x.

Henkel, C., Braatz, J. A., Menten, K. M., and Ott, J. (2008). "The kinetic temperature of a molecular cloud at redshift 0.9: ammonia in the gravitational lens PKS0-211." In: *A&A* 485, pp. 451–456 (cit. on p. 32).
DOI: 10.1051/0004-6361:20079140.

Henkel, C., Jethava, N., Kraus, A., Menten, K. M., Carilli, C. L., Grasshoff, M., Lubowich, D., and Reid, M. J. (2005). "The kinetic temperature of a molecular cloud at redshift 0.7: ammonia in the gravitational lens B0218+357." In: *A&A* 440, pp. 893–899 (cit. on p. 32).
DOI: 10.1051/0004-6361:20052816.

Henkel, C., Menten, K. M., Murphy, M. T., Jethava, N., Flambaum, V. V., Braatz, J. A., Muller, S., Ott, J., et al. (2009). "The density, the cosmic microwave background, and the proton-to-electron mass ratio in a cloud at redshift 0.9." In: *A&A* 500, pp. 725–734 (cit. on p. 28).
DOI: 10.1051/0004-6361/200811475.

Hodgman, S. S., R. G. Dall, L. J. Byron, K. G. H. Baldwin, S. J. Buckman, and A. G. Truscott (2009). "Metastable helium: a new determination of the longest atomic excited-state lifetime." In: *Phys. Rev. Lett.* 103, 053002 (cit. on p. 13).
DOI: 10.1103/PhysRevLett.103.053002.

Huntemann, N., B. Lipphardt, C. Tamm, V. Gerginov, S. Weyers, and E. Peik (2014). "Improved Limit on a Temporal Variation of m_p/m_e from Comparisons of Yb^{+} and Cs Atomic Clocks." In: *Phys. Rev. Lett.* 113, p. 210802 (cit. on pp. 26, 28).
DOI: 10.1103/PhysRevLett.113.210802.

Hutzler, N. R., H.-I. Lu, and J. M. Doyle (2012). "The Buffer Gas Beam: An Intense, Cold, and Slow Source for Atoms and Molecules." In: *Chemical Reviews* 112.9, pp. 4803–4827 (cit. on p. 36).
DOI: 10.1021/cr200362u.

Isaev, T. A. and R. Berger (2016). "Polyatomic Candidates for Cooling of Molecules with Lasers from Simple Theoretical Concepts." In: *Phys. Rev. Lett.* 116 (6), p. 063006 (cit. on p. 38).
DOI: 10.1103/PhysRevLett.116.063006.

Jansen, P., H. L. Bethlem, and W. Ubachs (2014). "Perspective: Tipping the scales: Search for drifting constants from molecular spectra." In: *J. Chem. Phys.* 140, 010901 (cit. on pp. 28, 29).
DOI: 10.1063/1.4853735.

Jansen, P., I. Kleiner, C. Meng, R. M. Lees, M. H. Janssen, W. Ubachs, and H. L. Bethlem (2013). "Prospects for high-resolution microwave spectroscopy of methanol in a Stark-deflected molecular beam." In: *Molecular Physics* 111.12-13, pp. 1923–1930 (cit. on p. 27).
DOI: 10.1080/00268976.2013.802819.

Jenč, F. (1983). "The Reduced Potential Curve Method for Diatomic Molecules and Its Applications." In: Advances in Atomic and Molecular Physics 19. Ed. by D. Bates and B. Bederson, pp. 265–307 (cit. on p. 30).
DOI: https://doi.org/10.1016/S0065-2199(08)60255-9.

Jenč, F., B. A. Brandt, V. Špirko, and O. Bludský (1993). "Estimation of the ground-state potentials of alkali-metal diatomic molecules with the use of the multiparameter generalized reduced-potential-curve method." In: *Phys. Rev. A* 48, pp. 1319–1327 (cit. on p. 30).
DOI: 10.1103/PhysRevA.48.1319.

Johnson, B. R. (1973). "The multichannel log-derivative method for scattering calculations." In: *Journal of Computational Physics* 13.3, pp. 445–449 (cit. on p. 40).
DOI: http://dx.doi.org/10.1016/0021-9991(73)90049-1.

Judd, B. R. and I. Lindgren (June 1961). "Theory of Zeeman Effect in the Ground Multiplets of Rare-Earth Atoms." In: *Phys. Rev.* 122 (6), pp. 1802–1812 (cit. on p. 48).
DOI: 10.1103/PhysRev.122.1802.

Juřek, M., V. Špirko, and W. P. Kraemer (1995). "Ab-initio determination of the rate coefficients for radiative association of $He(^1S) + H^+$." In: *Chem. Phys.* 193, pp. 287–296 (cit. on p. 14).
DOI: 10.1016/0301-0104(94)00428-D.

Kadau, H., M. Schmitt, M. Wenzel, C. Wink, T. Maier, I. Ferrier-Barbut, and T. Pfau (2016). "Observing the Rosensweig instability of a quantum ferrofluid." In: *Nature* 530.7589, pp. 194–197 (cit. on p. 46).
DOI: 10.1038/nature16485.

Kanekar, N. (2011). "Constraining changes in the proton-electron mass ratio with inversion and rotational lines." In: *The Astrophysical Journal* 728, p. L12 (cit. on p. 28).
DOI: 10.1088/2041-8205/728/1/l12.

Karremans, K., W. Vassen, and W. Hogervorst (1998). "Observation of the Transition to Chaos in the Level Statistics of Diamagnetic Helium." In: *Phys. Rev. Lett.* 81 (22), pp. 4843–4846 (cit. on p. 45).
DOI: 10.1103/PhysRevLett.81.4843.

Ketterle, W. and N. V. Druten (1996). "Evaporative Cooling of Trapped Atoms." In: *Advances In Atomic, Molecular, and Optical Physics* 37, pp. 181–236 (cit. on p. 37).
DOI: http://dx.doi.org/10.1016/S1049-250X(08)60101-9.

Koester, D. and G. Chanmugam (1990). "Physics of white dwarf stars." In: *Rep. Prog. Phys.* 837, p. 53 (cit. on p. 12).
DOI: 10.1088/0034-4885/53/7/001.

Kolbe, W. F., W. Zollner, and B. Leskovar (1981). "Microwave spectrometer for the detection of transient gaseous species." In: *Rev. Sci. Instrum.* 52.4, pp. 523–532 (cit. on p. 54).
DOI: 10.1063/1.1136633.

Kozlov, M. G. and S. A. Levshakov (2013). "Microwave and submillimeter molecular transitions and their dependence on fundamental constants." In: *Annalen der Physik* 525.7, pp. 452–471 (cit. on p. 28).
DOI: 10.1002/andp.201300010.

Kozyryev, I., L. Baum, K. Matsuda, B. L. Augenbraun, L. Anderegg, A. P. Sedlack, and J. M. Doyle (2017). "Sisyphus Laser Cooling of a Polyatomic Molecule." In: *Phys. Rev. Lett.* 118 (17), p. 173201 (cit. on p. 38).
DOI: 10.1103/PhysRevLett.118.173201.

Kozyryev, I., L. Baum, K. Matsuda, and J. M. Doyle (2016). "Proposal for Laser Cooling of Complex Polyatomic Molecules." In: *Chem. Phys. Chem* 17, pp. 3641–3648 (cit. on p. 36).
DOI: 10.1002/cphc.201601051.

Kreckel, H., H. Bruhns, M. Čížek, S. C. O. Glover, K. A. Miller, X. Urbain, and D. W. Savin (2010). "Experimental Results for H_2 Formation from H^- and H and Implications for First Star Formation." In: *Science* 329.5987, pp. 69–71 (cit. on p. 12).
DOI: 10.1126/science.1187191.

Krems, R. V. (2019). *Molecules in Electromagnetic Fields*. Hoboken, NJ: John Wiley and Sons, p. 483 (cit. on p. 36).

Kristiansen, P. and L. Veseth (1986). "Many-body calculations of hyperfine constants in diatomic molecules. II. First-row hydrides." In: *J. Chem. Phys.* 84.11, pp. 6336–6344 (cit. on p. 54).
DOI: 10.1063/1.450726.

Langhoff, S. R. and H. Partridge (1984). "Theoretical study of the Λ-doubling parameters for $X^2\Pi$ OH." In: *J. Mol. Spectrosc.* 105.2, pp. 261–275 (cit. on p. 54).
DOI: 10.1016/0022-2852(84)90217-0.

Leitner, D. M., R. S. Berry, and R. M. Whitnell (1989). "Quantum chaos of Ar_3: Statistics of eigenvalues." In: *The Journal of Chemical Physics* 91, pp. 3470–3476 (cit. on p. 45).
DOI: 10.1063/1.456876.

Lemarchand, C., M. Triki, B. Darquié, C. J. Bordé, C. Chardonnet, and C. Daussy (2011). "Progress towards an accurate determination of the Boltzmann constant by Doppler spectroscopy." In: *New Journal of Physics* 13.7, p. 073028 (cit. on p. 32).
DOI: 10.1088/1367-2630/13/7/073028.

Lepp, S., P. C. Stancil, and A. Dalgarno (2002). "Atomic and molecular processes in the early Universe." In: *J. Phys. B: At. Mol. Opt. Phys.* 35, R57–R80 (cit. on p. 12).
DOI: 10.1088/0953-4075/35/10/201.

Loo, M. P. J. van der and G. C. Groenenboom (2007). "Theoretical transition probabilities for the OH Meinel system." In: *J. Chem. Phys.* 126.11, p. 114314 (cit. on pp. 54, 56).
DOI: 10.1063/1.2646859.

Maier, T., I. Ferrier-Barbut, H. Kadau, M. Schmitt, M. Wenzel, C. Wink, T. Pfau, K. Jachymski, et al. (2015a). "Broad universal Feshbach resonances in the chaotic spectrum of dysprosium atoms." In: *Phys. Rev. A* 92 (6), p. 060702 (cit. on pp. 46, 48).
DOI: 10.1103/PhysRevA.92.060702.

Maier, T., H. Kadau, M. Schmitt, M. Wenzel, I. Ferrier-Barbut, T. Pfau, A. Frisch, S. Baier, et al. (2015b). "Emergence of Chaotic Scattering in Ultracold Er and Dy." In: *Phys. Rev. X* 5 (4), p. 041029 (cit. on pp. 46, 48, 49).
DOI: 10.1103/PhysRevX.5.041029.

Martí-Vidal, I., Muller, S., Combes, F., Aalto, S., Beelen, A., Darling, J., Guélin, M., Henkel, C., et al. (2013). "Probing the jet base of the blazar PKS0-211 from the chromatic variability of its lensed images - Serendipitous ALMA observations of a strong gamma-ray flare." In: *A&A* 558, A123 (cit. on p. 29).
DOI: 10.1051/0004-6361/201322131.

Mayle, M., B. P. Ruzic, and J. L. Bohn (2012). "Statistical aspects of ultracold resonant scattering." In: *Phys. Rev. A* 85 (6), p. 062712 (cit. on p. 46).
DOI: 10.1103/PhysRevA.85.062712.

McCarron, D. J., M. H. Steinecker, Y. Zhu, and D. DeMille (2018a). "Magnetic Trapping of an Ultracold Gas of Polar Molecules." In: *Phys. Rev. Lett.* 121 (1), p. 013202 (cit. on p. 36).
DOI: 10.1103/PhysRevLett.121.013202.

McCarron, D. J., M. H. Steinecker, Y. Zhu, and D. DeMille (2018b). "Magnetic Trapping of an Ultracold Gas of Polar Molecules." In: *Phys. Rev. Lett.* 121 (1), p. 013202 (cit. on p. 36).
DOI: 10.1103/PhysRevLett.121.013202.

Meerts, W. L. and A. Dymanus (1975). "A Molecular Beam Electric Resonance Study of the Hyperfine Λ Doubling Spectrum of OH, OD, SH, and SD." In: *Canadian Journal of Physics* 53.19, pp. 2123–2141 (cit. on p. 54).
DOI: 10.1139/p75-261.

Miranda, M. H. G. de, A. Chotia, B. Neyenhuis, D. Wang, G. Quéméner, S. Ospelkaus, J. L. Bohn, J. Ye, et al. (2011). "Controlling the quantum stereodynamics of ultracold bimolecular reactions." In: *Nature Physics* 7.6, pp. 502–507 (cit. on p. 46).
DOI: 10.1038/nphys1939.

Monroe, C. R., E. A. Cornell, C. A. Sackett, C. J. Myatt, and C. E. Wieman (Jan. 1993). "Measurement of Cs-Cs elastic scattering at T=30 μK." In: *Phys. Rev. Lett.* 70, pp. 414–417 (cit. on p. 37).
DOI: 10.1103/PhysRevLett.70.414.

Mrugała, F. and W. P. Kraemer (2005). "Radiative association of He^+ with H_2 at temperatures below 100 K." In: *J. Chem. Phys.* 122, 224321 (cit. on p. 14).
DOI: 10.1063/1.1924453.

Mrugała, F., V. Špirko, and W. P. Kraemer (2003). "Radiative association of HeH_2^+." In: *J. Chem. Phys.* 118, pp. 10547–10560 (cit. on p. 14).
DOI: 10.1063/1.1573184.

Mur-Petit, J. and R. A. Molina (Oct. 2015). "Spectral statistics of molecular resonances in erbium isotopes: How chaotic are they?" In: *Phys. Rev. E* 92 (4), p. 042906 (cit. on p. 49).
DOI: 10.1103/PhysRevE.92.042906.

Murphy, M. T., V. V. Flambaum, S. Muller, and C. Henkel (2008). "Strong Limit on a Variable Proton-to-Electron Mass Ratio from Molecules in the Distant Universe." In: *Science* 320, pp. 1611–1613 (cit. on p. 28).
DOI: 10.1126/science.1156352.

Ni, K. .-.-K., S. Ospelkaus, D. Wang, G. Quéméner, B. Neyenhuis, M. H. G. de Miranda, J. L. Bohn, J. Ye, et al. (2010). "Dipolar collisions of polar molecules in the quantum regime." In: *Nature* 464.7293, pp. 1324–1328 (cit. on p. 46).
DOI: 10.1038/nature08953.

Numerov, B. V. (1923). "Méthode nouvelle de la détermination des orbites et le calcul des éphémé rides en tenant compte des perturbations." In: *Trudy Glavnoi rossiiskoi astrofizicheskoi observatorii* 2, pp. 188–14 (cit. on p. 15).

Owens, A., S. N. Yurchenko, O. L. Polyansky, R. I. Ovsyannikov, W. Thiel, and V. Špirko (2015). "Accurate prediction of H_3O^+ and D_3O^+ sensitivity coefficients to probe a variable proton-to-electron mass ratio." In: *Monthly Notices of the Royal Astronomical Society* 454.3, pp. 2292–2298 (cit. on p. 28).
DOI: 10.1093/mnras/stv2023.

Owens, A., S. N. Yurchenko, and V. Špirko (2018). "Anomalous phosphine sensitivity coefficients as probes for a possible variation of the proton-to-electron mass ratio." In: *Monthly Notices of the Royal Astronomical Society* 473, pp. 4986–4992 (cit. on p. 28).
DOI: 10.1093/mnras/stx2696.

Owens, A., S. N. Yurchenko, W. Thiel, and V. Špirko (2016). "Enhanced sensitivity to a possible variation of the proton-to-electron mass ratio in ammonia." In: *Phys. Rev. A* 93, p. 052506 (cit. on p. 28).
DOI: 10.1103/PhysRevA.93.052506.

Patkowski, K., V. Špirko, and K. Szalewicz (2009). "On the Elusive Twelfth Vibrational State of Beryllium Dimer." In: 326.5958, pp. 1382–1384 (cit. on p. 30).
DOI: 10.1126/science.1181017.

Patrignani C. et al. (Particle Data Group) (2016). "Review of Particle Physics." In: *Chinese Physics C* 40.10, p. 100001 (cit. on p. 26).
DOI: 10.1088/1674-1137/40/10/100001.

Pérez-Ríos, J. and A. S. Sanz (2013). "How does a magnetic trap work?" In: *American Journal of Physics* 81, pp. 836–843 (cit. on p. 37).
DOI: 10.1119/1.4819167.

Pérez-Ríos, J., M. Lepers, R. Vexiau, N. Bouloufa-Maafa, and O. Dulieu (2014). "Progress toward ultracold chemistry: ultracold atomic and photonic collisions." In: *Journal of Physics: Conference Series* 488.1, p. 012031 (cit. on p. 46).
DOI: 10.1088/1742-6596/488/1/012031.

Perlmutter, S. (2012). "Nobel Lecture: Measuring the acceleration of the cosmic expansion using supernovae." In: *Rev. Mod. Phys.* 84 (3), pp. 1127–1149 (cit. on p. 26).
DOI: 10.1103/RevModPhys.84.1127.

Petrov, A., E. Tiesinga, and S. Kotochigova (2012). "Anisotropy-Induced Feshbach Resonances in a Quantum Dipolar Gas of Highly Magnetic Atoms." In: *Phys. Rev. Lett.* 109 (10), p. 103002 (cit. on p. 48).
DOI: 10.1103/PhysRevLett.109.103002.

Podolskiy, V. A. and E. E. Narimanov (2007). "Level spacing distribution in systems with partially chaotic classical dynamics." In: *Physics Letters A* 362.5, pp. 412–416 (cit. on p. 45).
DOI: 10.1016/j.physleta.2006.10.065.

Quéméner, G. and P. S. Julienne (2012). "Ultracold Molecules under Control!" In: *Chem. Rev.* 112.9, pp. 4949–5011 (cit. on p. 46).
DOI: 10.1021/cr300092g.

Quintero-Pérez, M., T. E. Wall, S. Hoekstra, and H. L. Bethlem (2014). "Preparation of an ultra-cold sample of ammonia molecules for precision measurements." In: *Journal of Molecular Spectroscopy* 300.

Spectroscopic Tests of Fundamental Physics, pp. 112–115 (cit. on p. 27).
DOI: https://doi.org/10.1016/j.jms.2014.03.018.

Radford, H. E. (1968). "Scanning Microwave Echo Box Spectrometer." In: *Rev. Sci. Instrum.* 39.11, pp. 1687–1691 (cit. on p. 54).
DOI: 10.1063/1.1683203.

Ramos, A. A. and J. T. Bueno (2006). "Theory and Modeling of the Zeeman and Paschen-Back Effects in Molecular Lines." In: *The Astrophysical Journal* 636, pp. 548–563 (cit. on p. 55).
DOI: 10.1086/497892.

Rothman, L. S., C. P. Rinsland, A. Goldman, S. T. Massie, D. P. Edwards, J.-M. Flaud, A. Perrin, C. Camy-Peyret, et al. (1998). "The HITRAN 2004 molecular spectroscopic database." In: *J. Quant. Spectrosc. Radiat. Transfer* 60, pp. 665–710 (cit. on p. 18).
DOI: 10.1016/S0022-4073(98)00078-8.

Safronova, M. S., D. Budker, D. DeMille, D. F. J. Kimball, A. Derevianko, and C. W. Clark (2018). "Search for new physics with atoms and molecules." In: *Rev. Mod. Phys.* 90 (2), p. 025008 (cit. on p. 26).
DOI: 10.1103/RevModPhys.90.025008.

Sakhr, J. and J. M. Nieminen (2005). "Poisson-to-Wigner crossover transition in the nearest-neighbor statistics of random points on fractals." In: *Phys. Rev. E* 72 (4), p. 045204 (cit. on p. 45).
DOI: 10.1103/PhysRevE.72.045204.

Semenov, M., S. N. Yurchenko, and J. Tennyson (2016). "Predicted Landé g-factors for open shell diatomic molecules." In: *J. Mol. Spectrosc.* 330. Potentiology and Spectroscopy in Honor of Robert Le Roy, pp. 57–62 (cit. on p. 53).
DOI: https://doi.org/10.1016/j.jms.2016.11.004.

Shelkovnikov, A., R. J. Butcher, C. Chardonnet, and A. Amy-Klein (2008). "Stability of the Proton-to-Electron Mass Ratio." In: *Phys. Rev. Lett.* 100 (15), p. 150801 (cit. on p. 27).
DOI: 10.1103/PhysRevLett.100.150801.

Shuman, E. S., J. F. Barry, and D. DeMille (2010). "Laser cooling of a diatomic molecule." In: *Nature* 467, pp. 820–823 (cit. on p. 36).
DOI: 10.1038/nature09443.

Soldán, P. and W. P. Kraemer (2012). "Molecular ion $LiHe^+$: *ab initio* study." In: *Chem. Phys.* 393, pp. 135–139 (cit. on p. 16).
DOI: 10.1016/j.chemphys.2011.11.040.

Spilker, J. S., M. Aravena, M. Béthermin, S. C. Chapman, C.-C. Chen, D. J. M. Cunningham, C. De Breuck, C. Dong, et al. (2018). "Fast molecular outflow from a dusty star-forming galaxy in the early Universe." In: 361.6406, pp. 1016–1019 (cit. on p. 33).
DOI: 10.1126/science.aap8900.

Špirko, V. (2014). "Highly Sensitive Ammonia Probes of a Variable Proton-to-Electron Mass Ratio." In: *J. Phys. Chem. Lett.* 5, pp. 919–923 (cit. on p. 28).
DOI: 10.1021/jz500163j.

Špirko, V. (2016). "Morphing ab initio potential energy curve of beryllium monohydride." In: *Journal of Molecular Spectroscopy* 330. Potentiology and Spectroscopy in Honor of Robert Le Roy, pp. 89–95 (cit. on pp. 30, 54).
DOI: https://doi.org/10.1016/j.jms.2016.08.009.

Stancil, P. C., J. F. Babb, and A. Dalgarno (1993). "The radiative association of He^+ and He and H^+ and H." In: *Astrophys. J.* 414, pp. 672–675 (cit. on p. 13).
DOI: 10.1086/173113.

Stancil, P. C. and A. Dalgarno (1997). "Stimulated radiative association of Li and H in the early Universe." In: *Astrophys. J.* 479, pp. 543–546 (cit. on pp. 15, 16).
DOI: 10.1086/303920.

Stuhl, B. K., M. T. Hummon, M. Yeo, G. Quéméner, J. L. Bohn, and J. Ye (2012). "Evaporative cooling of the dipolar hydroxyl radical." In: *Nature* 492, pp. 396–400 (cit. on p. 40).
DOI: 10.1038/nature11718.

Swings, P. (1942). "Considerations regarding cometary and interstellar molecules." In: *Astrophys. J.* 95, pp. 270–280 (cit. on p. 13).
DOI: 10.1086/144393.

Talbi, D. and M.-C. Bacchus-Montabonel (2007). "Formation of HF through radiative association in the early universe." In: *Chem. Phys. Lett.* 443, pp. 40–42 (cit. on p. 14).
DOI: 10.1016/j.cplett.2007.06.071.

Ter Meulen, J. J. and A. Dymanus (1972). "Beam-Maser Measurements of the Ground-State Transition Frequencies of OH." In: *Astrophys. J. Lett.* 172, p. L21 (cit. on p. 54).
DOI: 10.1086/180882.

Ter Meulen, J. J., W. L. Meerts, G. W. M. van Mierlo, and A. Dymanus (1976). "Observations of Population Inversion between the Λ-Doublet States of OH." In: *Phys. Rev. Lett.* 36 (17), pp. 1031–1034 (cit. on p. 54).
DOI: 10.1103/PhysRevLett.36.1031.

Tielens, A. G. G. M. (2013). "The molecular universe." In: *Rev. Mod. Phys.* 85, pp. 1021–1081 (cit. on p. 12).
DOI: 10.1103/RevModPhys.85.1021.

Ubachs, W., J. Bagdonaite, E. J. Salumbides, M. T. Murphy, and L. Kaper (2016). "Colloquium: Search for a drifting proton-electron mass ratio from H_2." In: *Rev. Mod. Phys.* 88, p. 021003 (cit. on p. 28).
DOI: 10.1103/RevModPhys.88.021003.

Uzan, J.-P. (2011). "Varying Constants, Gravitation and Cosmology." In: *Living Reviews in Relativity* 14.1, p. 2 (cit. on p. 26).
DOI: 10.12942/lrr-2011-2.

Varberg, T. and K. Evenson (1993). "The Rotational Spectrum of OH in the $v = 0 - 3$ Levels of Its Ground State." In: *J. Mol. Spectrosc.* 157.1, pp. 55–67 (cit. on p. 54).
DOI: https://doi.org/10.1006/jmsp.1993.1005.

Varberg, T. D., F. Stroh, and K. M. Evenson (1999). "Far-Infrared Rotational and Fine-Structure Transition Frequencies and Molecular Constants of ^{14}NO and ^{15}NO in the $X^2\Pi$ $(v = 0)$ State." In: *Journal of Molecular Spectroscopy* 196.1, pp. 5–13 (cit. on p. 38).
DOI: http://dx.doi.org/10.1006/jmsp.1999.7850.

Vogels, S. N., J. Onvlee, S. Chefdeville, A. van der Avoird, G. C. Groenenboom, and S. Y. T. van de Meerakker (2015). "Imaging resonances in low-energy NO-He inelastic collisions." In: *Science* 350, p. 787 (cit. on p. 40).
DOI: 10.1126/science.aad2356.

Wang, Y., J. P. D'Incao, and C. H. Greene (2011). "Universal Three-Body Physics for Fermionic Dipoles." In: *Phys. Rev. Lett.* 107 (23), p. 233201 (cit. on p. 46).
DOI: 10.1103/PhysRevLett.107.233201.

Wigner, E. P. (1955). "Characteristic Vectors of Bordered Matrices With Infinite Dimensions." In: *Annals of Mathematics* 62.3, pp. 548–564 (cit. on pp. 45, 49).
DOI: 10.2307/1970079.

Williams, H. J., L. Caldwell, N. J. Fitch, S. Truppe, J. Rodewald, E. A. Hinds, B. E. Sauer, and M. R. Tarbutt (2018). "Magnetic Trapping and Coherent Control of Laser-Cooled Molecules." In: *Phys. Rev. Lett.* 120 (16), p. 163201 (cit. on p. 36).
DOI: 10.1103/PhysRevLett.120.163201.

Yang, B. C., J. Pérez-Ríos, and F. Robicheaux (Apr. 2017). "Classical Fractals and Quantum Chaos in Ultracold Dipolar Collisions." In: *Phys. Rev. Lett.* 118 (15), p. 154101 (cit. on pp. 46, 48).
DOI: 10.1103/PhysRevLett.118.154101.

Yelin, S. F., K. Kirby, and R. Côté (2006). "Schemes for robust quantum computation with polar molecules." In: *Phys. Rev. A* 74 (5), p. 050301 (cit. on p. 46).
DOI: 10.1103/PhysRevA.74.050301.

Yeo, M., M. T. Hummon, A. L. Collopy, B. Yan, B. Hemmerling, E. Chae, J. M. Doyle, and J. Ye (2015). "Rotational State Microwave Mixing for Laser Cooling of Complex Diatomic Molecules." In: *Phys. Rev. Lett.* 114, p. 223003 (cit. on p. 36).
DOI: 10.1103/PhysRevLett.114.223003.

Yurchenko, S. N., L. Lodi, J. Tennyson, and A. V. Stolyarov (2016). "Duo: A general program for calculating spectra of diatomic

molecules." In: *Computer Physics Communications* 202, pp. 262–275 (cit. on p. 53).
DOI: https://doi.org/10.1016/j.cpc.2015.12.021.

Zámečníková, M., L. Augustovičová, W. P. Kraemer, and P. Soldán (2015). "Formation of molecular ion $LiHe^+$ by radiative association of metastable helium $He(2^3P)$ with lithium ions." In: *Journal of Physics: Conference Series* 635, p. 022038 (cit. on p. 14).
DOI: 10.1088/1742-6596/635/2/022038.

Życzkowski, K., M. Lewenstein, M. Kuś, and F. Izrailev (1992). "Eigenvector statistics of random band matrices." In: *Phys. Rev. A* 45 (2), pp. 811–815 (cit. on p. 49).
DOI: 11.1103/PhysRevA.45.811.

Zygelman, B. and A. Dalgarno (1990). "The radiative association of He^+ and H." In: *Astrophys. J.* 365, pp. 239–240 (cit. on pp. 14, 16).
DOI: 10.1086/169475.

Zygelman, B., A. Dalgarno, M. Kimura, and N. F. Lane (1989). "Radiative and nonradiative charge transfer in He^+ + H collisions at low energy." In: *Phys. Rev. A* 40, pp. 2340–2345 (cit. on p. 19).
DOI: 10.1103/PhysRevA.40.2340.

Zygelman, B., P. C. Stancil, and A. Dalgarno (1998). "Stimulated radiative association of He and H^+." In: *Astrophys. J.* 508, pp. 151–156 (cit. on p. 14).
DOI: 10.1086/306399.